frontiers | Frontiers in Materials

TYPE Original Research
PUBLISHED 08 January 2024
DOI 10.3389/fmats.2023.1293254

OPEN ACCESS

EDITED BY
Alberto Corigliano,
Polytechnic University of Milan, Italy

REVIEWED BY
Kailu Xiao,
Texas A and M University, United States
Uthayakumar Marimuthu,
Kalasalingam University, India
Mustafa Kuntoğlu,
Selcuk University, Türkiye

*CORRESPONDENCE
Shubham Sharma,
shubham543sharma@gmail.com
Rajeev Kumar,
rajeev14584@lpu.co.in
Baljeet Singh,
baljeet.sliet@gmail.com

†These authors have contributed equally to this work

RECEIVED 12 September 2023
ACCEPTED 22 November 2023
PUBLISHED 08 January 2024

CITATION
Singh B, Singh Grewal J, Kumar R, Sharma S, Kumar A, Mohammed KA, Awwad FA, Khan MI and Ismail EAA (2024), Novel study on investigating the mechanical, microstructure morphological, and dry sliding wear characteristics of grey cast iron GG25 with copper additions for valve guides in internal combustion engine. *Front. Mater.* 10:1293254. doi: 10.3389/fmats.2023.1293254

Novel study on investigating the mechanical, microstructure morphological, and dry sliding wear characteristics of grey cast iron GG25 with copper additions for valve guides in internal combustion engine

Baljeet Singh[1*†], Jasmaninder Singh Grewal[2], Rajeev Kumar[3*], Shubham Sharma[4,5,6*†], Abhinav Kumar[7], Kahtan A. Mohammed[8,9], Fuad A. Awwad[10], M. Ijaz Khan[6,11] and Emad A. A. Ismail[10]

[1]Mechanical Engineering Department, Punjab Technical University, Jalandhar, India, [2]Department of Mechanical and Production Engineering, Guru Nanak Dev Engineering College, Ludhiana, India, [3]School of Mechanical Engineering, Lovely Professional University, Phagwara, India, [4]School of Mechanical and Automotive Engineering, Qingdao University of Technology, Qingdao, China, [5]Centre of Research Impact and Outcome, Chitkara University Institute of Engineering and Technology, Chitkara University, Rajpura, Punjab, India, [6]Department of Mechanical Engineering, Lebanese American University, Kraytem, Beirut, Lebanon, [7]Department of Nuclear and Renewable Energy, Ural Federal University Named After The First President of Russia, Yekaterinburg, Russia, [8]Faculty of Pharmacy, Jabir Ibn Hayyan Medical University, Najaf, Iraq, [9]Department of Medical Physics, Hilla University College, Babylon, Iraq, [10]Department of Quantitative Analysis, College of Business Administration, King Saud University, Riyadh, Saudi Arabia, [11]Department of Mechanics and Engineering Science, Peking University, Beijing, China

Introduction: The performance functionality efficacy of the engine's valve train assembly is considerably affected by the valve guide. Material selection is impacted by the prolonged operational lifespan of engines, which favours casting and machining materials such as cast iron. The intent of this study is to examine the dry sliding characteristics of GG25 cast iron with copper additives. Discovering the ways in which variations in load and sliding velocity impact wear characteristics is of paramount significance.

Methods: The research entailed the examination of wear characteristics across various environmental conditions. Loads were varied at 30 N, 40 N, and 50 N while maintaining a 1 m/s velocity constant. In the same manner, sliding velocities of 0.5 m/s, 1 m/s, and 2 m/s were varied while a constant load of 30 N was maintained. Experimental techniques were carried out at ambient temperature. Throughout the investigations, frictional forces and the coefficient of friction were also determined. The wear mechanisms of samples that had become deteriorated or worn-out were examined by employing a scanning electron microscope when combined with EDX analysis.

Results: A rise in the normal load from 30 N to 40 N led to a twofold rise in wear losses, measuring 417 microns as compared with 222 microns previously. The range of wear losses observed at moderate speeds (0.5 m/s–1 m/s) was 133–222 microns. Conversely, the maximum wear loss observed was 1,226 microns at elevated sliding velocities of 2 m/s, in contrast to 617 microns at higher normal loads of 50 N.

Additionally, the research discovered that normal load is more pronounced when both loading and speed are moderate, whereas sliding speed becomes more substantial when both are raised, culminating to higher wear losses.

Discussions: In summary, the research highlights the considerable effect that normal load and sliding speed have on the prevalence of wear losses. In conditions of moderate loading and velocity, the influence of normal load is more significant. However, as sliding accelerates, it becomes the predominant factor. An analysis of frictional forces as well as the coefficient of friction indicated that under loading conditions of 30 N–50 N, the friction coefficient raised from 0.238 to 0.43. The wear mechanisms, as discerned via scanning electron microscopy and EDX analysis, underscored the considerable impact of increased sliding velocity on wear loss in comparison to conditions of higher loading.

KEYWORDS

grey cast iron, GG25, valve guides, wear, ferrous, pin on disc, SEM, XRD

1 Introduction

Valve guide wear is a serious problem found over the years. In the internal combustion engine, these tubular elements serve as axial bearings for the engine poppet valves. It is the function of the valve guide to bear transverse loads that can damage the valve stem. The grey cast iron material due to its better sliding and wear characteristics is crucial in defining the wear performance of the valve guides under severe strain conditions. The rising demand for minimal exhaust emissions thanks to RDE, CAFÉ, and Euro norms, the continuous reductions in the sulphur levels of fuels, and flex fuels engines together all have a significant effect on valve and seat insert wear (Ramakrishnan, 2013). Lower content of sulphur in the fuels tends to decrease the lubricity which further exaggerates the wear on various engine components including valve guides. Data adjustments in ECU are chiefly employed to improve the power and torque characteristics without increasing the specific fuel consumption (Synák et al., 2019). Design engineers tend to increase the compression ratios in order to improve the power of the engines. It has been experimentally found that a 16:1 compression ratio yields the best performance at minimum specific fuel composition (Milojević et al., 2022). One more approach is to minimize these losses is by improving tribological characteristics between the sliding components. Novel materials with improved mechanical properties and self-lubricating properties can be helpful in this situation. AlSi10Mg was reinforced with cast iron. It has been concluded that friction coefficient values were a minimum of 0.231 for reinforced alloy AlSi10Mg in comparison to 0.350 for plain ALSi10Mg alloy (Milojević et al., 2023).

Hence, in order to increase the corporate average fuel economy manufactures are always in demand of new materials with minimal wear in the engines. Valve guide wear depends upon several factors including load, speed, temperature, lubrication, and composition. A new valve guide material with composition C 3.5%, Si 2%, Mn 0.7%, P 0.8%, Cr 0.2%, and rest Fe has been tested for wear characteristics. It has been found that the alloy was having wear resistance to 600°C. However, this composition suffers from machinability problems. Also, if alternate fuels are used this alloy is affected by corrosion (Skrbek and Mráz, 2020). A new material for the valve guide has been developed with a composition of 0.9% Al, 0.3% C, and the rest Cu. The wear results were compared with the existing valve guide material Gh1051. It was found that the wear rate of the new material is 2.8 times less than the existing vale guide material Gh1051. This has been attributed to the formation of γ-Al_2O_3 nano dispersed phases in the matrix resulting in improved mechanical properties (Vladimirova and Shalunov, 2020). Al-SiC (5%–30%) composites were fabricated for a novel valve guide material. It has been concluded that the hardness and wear resistance of developed composite increased with increasing SiC percentage and can replace the existing grey cast iron material (Purohit and Sagar, 2010). A comparative study has been done for different valve guide materials like Al-SiC, Ti-834, and CuNi3Si. It has been found that the stresses were least in the case of Al-SiC material and can be used as valve guide material (Srivastva et al., 2016). Efforts have been made to see the effects of all these factors in grey cast iron material as this is the most used material for the manufacturing of valve guides.

Grey cast iron chiefly finds its applications in situations where it is difficult to get lubricated conditions such as in internal combustion engines, especially in the valves and valve guides. Due to the continuous reciprocating action of the valve in the valve guides adequate lubricated conditions cannot be maintained. However, as grey cast iron contains about three to four wt% C and most of the carbon is present in the form of graphite flakes or nodules, this serves to provide the demanded lubricated effect in such tough conditions (Scherge et al., 2015). Grey cast iron exists in pearlite form. It is well known that the ferrite structure is believed to be soft and hence aids in minimizing wear (Terheci et al., 1995).

It is important to use appropriate materials to reduce the amount of wear and tear caused by dry sliding wear in various industrial applications. As a result of its unique properties, the cast iron grade GG25 is widely employed in dry sliding wear tests due to its excellent wear resistance. In dry sliding wear tests, cast iron grade GG25 is of particular importance and can be applied in the following ways.

Tribology is the science that studies friction, wear, and lubrication between surfaces when they interact with one another. There are several advantages that make cast iron grade GG25 an important material for tribological studies, such as its high wear resistance, low coefficient of friction, and ease of machining. During the design and selection process of materials for industrial applications, tribology studies are imperative.

In the automotive industry, cast iron grade GG25 is widely used for the manufacture of brake discs and other components susceptible to dry sliding wear. In addition to improving the

braking performance, GG25 also reduces wear, which results in a longer service life for brake discs.

Machine tools and other components subjected to dry sliding wear are also produced with cast iron grade GG25 in the manufacturing industry. In addition to improving machine tool durability, GG25 reduces wear and improves the quality of manufactured goods.

It is imperative that cast iron grade GG25 be used in dry sliding wear tests in order to achieve the best results for research and development. GG25 can be used to develop new materials with improved wear resistance and other properties by studying its wear behavior under different conditions and parameters. As a result of its excellent properties, cast iron grade GG25 is an extremely versatile material that finds application in a variety of industrial applications. In dry sliding wear tests, where appropriate materials are required to reduce wear and tear, it is ideal for use as a dry sliding wear test material because of its unique properties. As a result of its use in tribological studies, automotive, and manufacturing industries, as well as research and development, GG25 is an extremely valuable and significant material.

Cast iron GG25 has excellent wear- and heat-resistant properties, and the sliding motion of valves against the valve guides causes friction and wear, so using a material like cast iron that has self-lubricating properties due to the presence of graphite flakes contributes to improving the lifespan of the valve guides. Secondly, copper has been introduced up to a limited extent in order to promote the formation of a fine pearlite matrix. This contributes to improved mechanical properties like hardness. However, more copper addition is limited to the fact that it inhibits the growth of graphite flakes and thus affects solid lubricating properties. Other advantages include compatibility of cast iron GG25 with other materials such as stainless steel, alloy steels, etc., and economical production and vibration-dampening characteristics.

The effect of phosphorus 0.2% and 1% in grey cast iron has been investigated. Results showed that it leads to the development of a phosphide network and strengthens the metal matrix (Milojević et al., 2023). The effect of varying percentages of phosphorus in grey cast iron matrix in dry sliding conditions has been observed. It is apprised that severe wear losses occurred at the lowest level of 0.2 wt % P iron occurred at all loading conditions (Campbell et al., 1996). Medium-grade type-A graphite flakes enable as well as influence the movement of crack propagation. It starts with delamination leads to crack formation and finally shows the signs of scuffing–a severe form of adhesive wear (Vadiraj et al., 2010). It has been found that the hypereutectic gray irons studied have a higher graphite volume fraction (20%) with Type-A graphite flake morphology resulting in reduced wear rates (Prasad, 2011). Tensile strength as well as wear rates exhibit reduced values with an increase in graphite formation in the cast iron matrix (Vadiraj et al., 2011). Wear tests of hypoeutectic grey cast iron revealed that wear resistance is attributed to the presence of a combination of hard carbides and the softer graphite flakes present in the wear testing of hypoeutectic grey cast iron (Riahi and Alpas, 2003; Kowandy et al., 2007).

Wear behavior for A30 grey cast iron has been studied and a wear map was constructed. Certain necks are formed, leading to the formation of large-size debris in the gray cast iron matrix (Ferreira, 2002). Two self-lubricating materials PTFE and graphite were wear-tested against cast iron EN- GFL 250. The wear rate was less in the case of graphite solid lubricant up to 450°C while humidity has no effect on PTFE solid lubricant (Masuda et al., 2021). Grey cast iron and 1,080 steel were subjected to scuffing tests. The experimental observations exhibited that the scuffing behavior initiates the crack propagation for grey iron and plastic deformation of the matrix in the case of 1,080 steel (Singh et al., 2021a). It is apprised that the wear rate is reduced with the additions of manganese and chromium in the grey cast iron matrix (Vadiraj et al., 2011). It has been reported that graphite in the boride samples further prevents crack propagation in the hard boride samples and acts as a solid lubricant and minimizes wear (Sipcikoğlu et al., 2015). Cast iron SAE J431 was subjected to chilling heat treatment and another group of samples were carburized. It was found that chilled cast iron showed a reduction in wear rate and minimum friction coefficient and saved machining costs as carburized samples are difficult to machine (Abdou et al., 2018). It was found that at low speeds the graphite smears on the surface of mating components which prevents metal-to-metal contact and minimizes friction (Zhou et al., 2021). Wear mechanisms and the wear behaviour of single- and dual-step Austenite ductile iron are reviewed. The combination of a finely developed au ferritic microstructure and a hardened surface is thought to provide austenite ductile iron with better wear resistance (Alemani et al., 2017). The friction and wear behaviour of ductile iron and austempered grey cast iron were investigated. It has been discovered that when material hardness increases, the coefficient of friction in austempered grey cast iron becomes steadier and higher (García et al., 2018). Investigation has been done on the effects of sliding speed, and moisture content on the wear of graphite against cast iron. Cast iron surfaces were shielded from wear when graphite was smeared on top of them. It is found that when sliding conditions were significantly altered, the wear mode shift from severe to mild or *vice versa* led to a significant disparity in the wear of cast iron (Kumar et al., 2022a). Cast iron, brake blocks tribology at low temperatures has been studied using pin-on-disc technology. Due to the low durability of iron-based materials at low temperatures, cast iron brakes have been shown to wear down quickly. Furthermore, as cast iron's worn graphite transforms into a solid lubricant, the friction coefficient is decreased (Chawla et al., 2013). Investigations were done on the wear properties of grey cast iron, AISI NO.35B (JIS FC250). It has been discovered that CoF is constant for all loads below 40 N and drops to 0.004 when the load exceeds 40 N (Kumar et al., 2022b). Graphite addition in the Al 6061-T6 matrix results in an improvement of yield strength and hardness. Further, graphite addition improved machinability and uniform distribution of reinforcements in the matrix due to enhanced wettability (Kumar et al., 2023a). The friction coefficient and wear losses of grey cast iron crankshaft bearings mated with austempered and MnP-coated ductile cast iron have been experimentally examined under both dry and boundary lubrication situations under various speed and load conditions. According to reports, the friction coefficient drops as the normal load rises. CoF is not significantly affected as the sliding speed rises (Jain et al., 2023).

Incorrect valve seating can result from worn valve guides, which leave too much gap between the valve stem and the guide. Valve leakage that causes compression loss can also result in engine misfires. The guides quickly deteriorate due to the constant contact between the stem and the guide. In this study, the effect

of copper on GG25 and the effect of low phosphorus content have been studied. Copper's addition results in improved mechanical properties leading to minimized wear and friction coefficient. Secondly, low phosphorus content reduces brittleness and improves toughness resulting in minimizing the fracturing of the matrix under stress. It improves machinability as no phosphide networks (hard phases) are formed. It also provides resistance to embrittlement and corrosion resistance. Combined, the addition of copper and limiting phosphorus improves the life span of the components with improved mechanical properties.

The key to the functioning of the valve train assembly, the valve guide has a substantial implication on the performance of the engine. With regard to its superior casting and machining characteristics, cast iron, specifically the GG25 grade, is the material of choice for valve guides. The objective of this research is to explore the dry sliding characteristics of GG25, which has been enriched with copper additives. By performing this, the article promises to offer insights into the wear characteristics of GG25 at distinct loads and sliding velocities. The study examines the impacts that normal load and sliding speed have on frictional forces, wear mechanisms, and wear losses. Furthermore, the research investigates the mechanical characteristics, metallographic examination, as well as XRD analysis of GG25 when copper is incorporated, thereby offering valuable perspectives on its performance across various scenarios.

The practicable applications, significance, as well as scientific novelty have been elucidated as follows.

i. **Mechanical Characteristics Enhancement:** The findings of the research indicate that the incorporation of copper into GG25 leads to an enhancement of its mechanical characteristics. By refining the pearlite matrix, hardness and compressive strength are enhanced. A reduced phosphorus content is associated with enhanced durability and ductility, both of which are vital for engine applications requiring longevity.
ii. **Metallographic and XRD Analyses:** The microstructure of GG25 with copper additions is revealed through the utilisation of Olympus micro-image software and XRD analysis. The formation of fine pearlite is facilitated by copper, and as its concentration increases, the presence of graphite reduces. Enhanced durability as well as resistance to wear are outcomes of this refined microstructure.
iii. **Wear Behavior Insights:** The study provides a thorough analysis of the wear behaviour of GG25, which incorporates copper, when subjected to different sliding velocities and pressures. This study reveals the implications of sliding speed and normal load on wear rates, friction coefficients, and wear mechanisms. The findings of the research offer significant knowledge for the design of engine components that possess enhanced longevity, and durability.
iv. **Temperature Sensitivity of Graphite Layers:** The study explores the sensitivity of graphite layers to temperature, with the goal of delineating their purpose in reducing wear. The study illustrates how a rise in temperature causes graphite layers to smear, functioning as a lubricating film. Comprehending this temperature-dependent behaviour is of paramount significance in order to optimise engine efficiency and mitigate wear-related challenges.
v. **Practical Implications for Engine Design:** The findings emphasise the significance of incorporating graphite into GG25, which serves as a solid lubricant. The real-world operational practical implications of this highlight the significance of incorporating load, sliding speed, as well as temperature into the engine's design in order to enhance performance in general along with resistance to wear. Developing design modifications upon these insights could culminate in components for engine parts that are more robust, durable, resilient, and efficient.

TABLE 1 Constituent Elements of cast iron GG25 Samples.

Elements	Actual %
Carbon (C)	3.20%
Copper (Cu)	2.40%
Silicon (Si)	2.10%
Manganese (Mn)	0.60%
Sulphur (S)	0.12%
Phosphorus (P)	0.15%
Iron (Fe)	Remaining

In summary, this research provides novel insights by examining the dry sliding behaviour of GG25 when copper is incorporated. As a consequence, a thorough comprehension of the material's mechanical properties, wear characteristics, and microstructural changes is achieved. The practical implications encompass the optimisation of engine design with the goal of accomplishing enhanced performance, durability, and resistance to wear in real-life applications.

Hence, in the present study, the wear performance of grey cast iron grade GG25 pin samples has been tested in a dry sliding medium. Further, copper has been added to promote a fine pearlite matrix. This study will apprise the effect of copper addition in grey cast iron GG25 in wear characteristics, and the scope of the use of this material in valve guide applications.

2 Materials and methods

2.1 Material

In this study, cast iron grade GG25 is selected for dry sliding wear behavior. It is added with a small amount of copper and limited phosphorus content. Sand casting is used to produce the blanks for cast iron guides. Induction furnaces were used to melt the cast iron GG25 and copper up to 2.40% is added at this stage. Copper powder was preheated to remove any moisture. Samples are cast in the form of solid bars. The blanks are then machined to achieve the required dimensions and geometrical shape. A total of 5 samples were prepared with elemental composition (in mass%) of the sample as mentioned below in Table 1.

Before the experimentation, these samples were sponged with acetone to remove any dirt grease, etc. Further polishing is done with

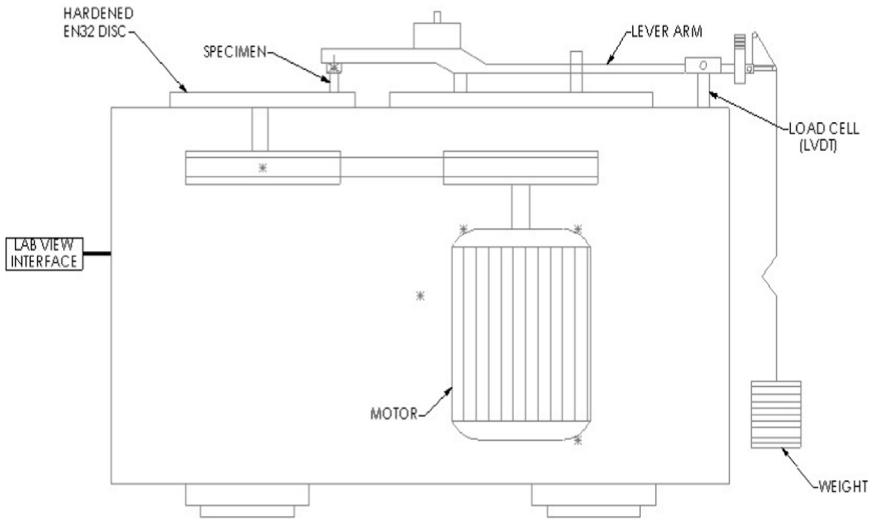

FIGURE 1
Tribometer test-rig.

emery papers of 600, 800, and 1,000 to remove the rust. One end of the pins was ground to make a flat surface with rounded edges. The flat surface of the sample pins ensures proper contact with the hardened disc surface during sliding. Also, the round edges of the pins ensure no biting up due to the sharp edges of the samples, and that safeguards the hardened disc.

2.2 Characterizations

The surface analysis and the number of phases developed in the worn-out cast iron GG25 samples were examined with FESEM coupled with an EDX detector, Carl Zeiss-Model Gemini. The XRD imaging of as cast GG25 sample was exhibited with a scanning range of 20°–160°, Bruker D8 advance.

The porosity of the GG25 cast iron samples with Cu addition was calculated by area-fraction technique using an optical microscope coupled with Image J analytical software. Micro hardness measurement was carried out as per ASTM E384:2011. The tensile, and compressive strengths were also measured as per ASTM E8-95 Standards.

2.3 Wear test

Intake and exhaust valve stems of internal combustion engines slide against the valve guides at specific normal loads, sliding speeds, and lubrication conditions. During the running of an engine, valve guides are subjected to wear and friction. A pin on disc apparatus easily simulates these conditions under controlled loads and speeds to study the tribological behavior of the components.

Experimental trials under dry-sliding wear conditions have been conducted as per ASTM G99 standards, pin on disc, Ducom Instrument Ltd. as shown in Figure 1 in order to make comparisons with the reviewed literature, which also used the pin-on-disc testing configuration.

TABLE 2 Test parameters.

Test parameters	Range
Sliding Speed	0.5 m/s, 1 m/s and 2 m/s
Sliding distance	5400 m
Applied load	30 N, 40 N and 50 N
Time	90 min

The grey cast iron GG25 pin samples φ 12 mm × 35 mm were slid against a hardened disc of EN32, R_a value 0.3–0.5 μm. Before the start of each experimental trial, it was ensured to degrease the pin sample as well as the hardened disc with acetone to phase out any possible impurities.

The wear loss estimation has been done with a linear variable differential transducer (LVDT). The dead weight put on the load panel further multiplies the load on the pin sample via lever action. At the end of each experimental test run, pin samples were weighed with an electronic weighing balance (0.001 mg).

Valve guides are subjected to loads from valve stems during the opening and closing of valves and also from valve springs. As available from the literature, load values vary from 10 N to 50 N, and sliding speed varies from 0.1–1 m/s and depends upon the capacity of the engines and the engine speeds. In the present study, load condition varies from 30, 40, and 50 N and sliding speed varies from 0.5, 1, and 2 m/s. The test parameters are given in Table 2.

3 Results and discussions

3.1 Characterization of GG25 +Cu Sample

The SEM images shown in Figure 2 depict the surface morphology of the as-casted GG25 samples with Cu additions. It is further verified from the SEM image that there is negligible

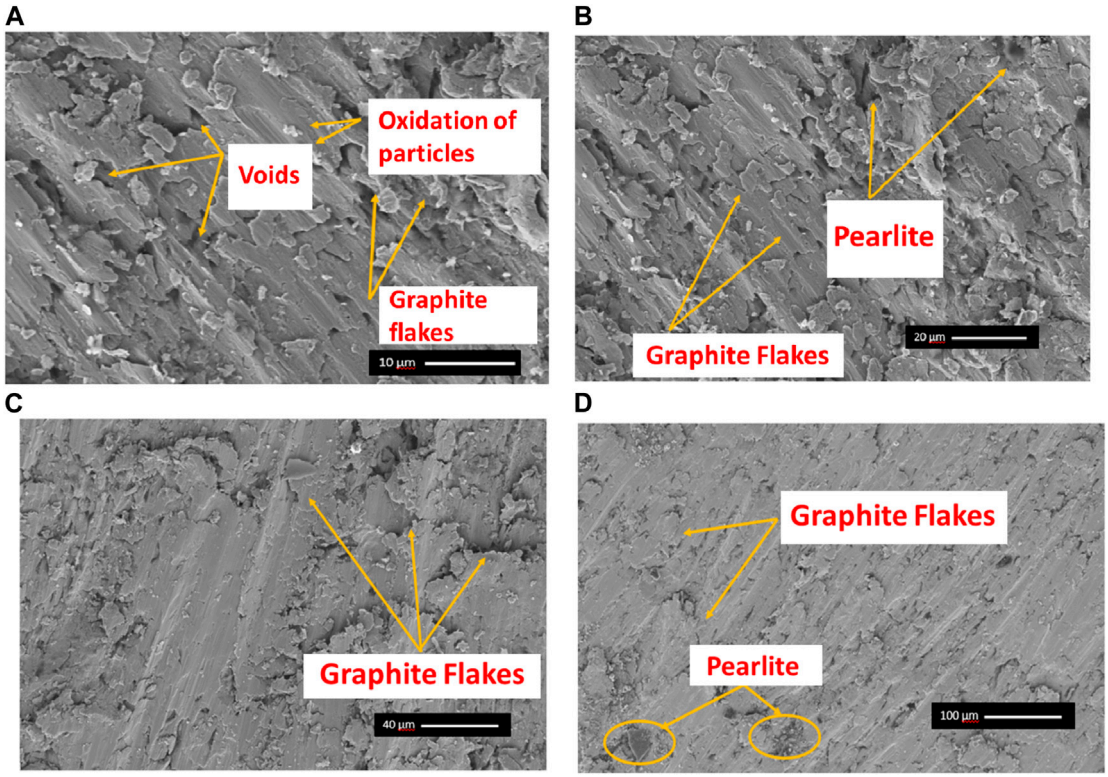

FIGURE 2
(A–D) SEM micrographs of casted GG25+Cu sample.

oxidation of particles and no chemical reactions with oxygen resulting in uniform lamellas of graphite in the entire matrix. The distribution and shape of the graphite change along with the Cu in grey iron. As a result, grey iron's tensile strength and hardness increase significantly. Many researches claim that even a small amount of copper improves the mechanical properties. As a result, copper is a crucial component in the production of grey iron.

It promotes the growth of graphite and quickens pearlite development. The development of pearlite as a result of copper addition makes grey cast iron stronger. Additionally, in low carbon steels' corrosion is greatly reduced by less than 1% of copper. However, there is a big impact on the characteristics from the difference in Cu %. The pearlite is formed when copper refines the graphite flakes. Ferrite is transformed by copper into a pearlite matrix. The mechanical properties, especially wear resistance and hardness, are significantly improved. Copper coarsens and stabilises graphite while increasing the number of eutectic cells and decreasing their size. Strength is less affected when copper percentage rises. The surface area of graphite flakes is reduced by copper (Sharma et al., 2023).

3.2 Effect on mechanical properties of GG25 with copper addition

In ferrous-based materials, carbon is the main component of the interstitial strengthening process. The mechanical qualities are developed as the amount of carbon increases (hardness, strength) within the matrix. On the other hand, it is possible to imagine a fully pearlitic matrix as a precipitation-hardened matrix with lamellar-shaped ferrite, and cementite phases (Gill et al., 2020).

The interlamellar spacing of pearlite has a significant impact on its strength, as is well recognised from physical metallurgy principles. The strength (hardness) of the matrix increases as the spacing decreases as depicted in Figure 3.

While copper encourages the formation of the austenite structure and the pearlite structure. Additionally, it helps the graphite structure a little. Graphite flakes get smaller in size as the copper content of grey cast iron increases (Kumar et al., 2023b).

Low phosphorus content improves toughness, improves ductility. This contributed to an increase in the tensile strength of the cast alloy. Secondly, copper addition promotes the formation of a fine pearlite matrix resulting in improved hardness. This is evident from the increases compressive strength value obtained during the compression tests conducted on the cast samples GG25.

3.3 Metallographic analysis

The automatic system Olympus micro-image software was used to do the quantitative metallographic analysis for the purpose of measuring porosity. The value of porosity as depicted in Table 3 shows that there is negligible oxidation during the pouring of metal in the mold. GG25 with copper additions sample was polished using emery paper with grit sizes of 180, 240, 320, 400, and 600. The specimen is then polished on a disc polishing machine using 6-

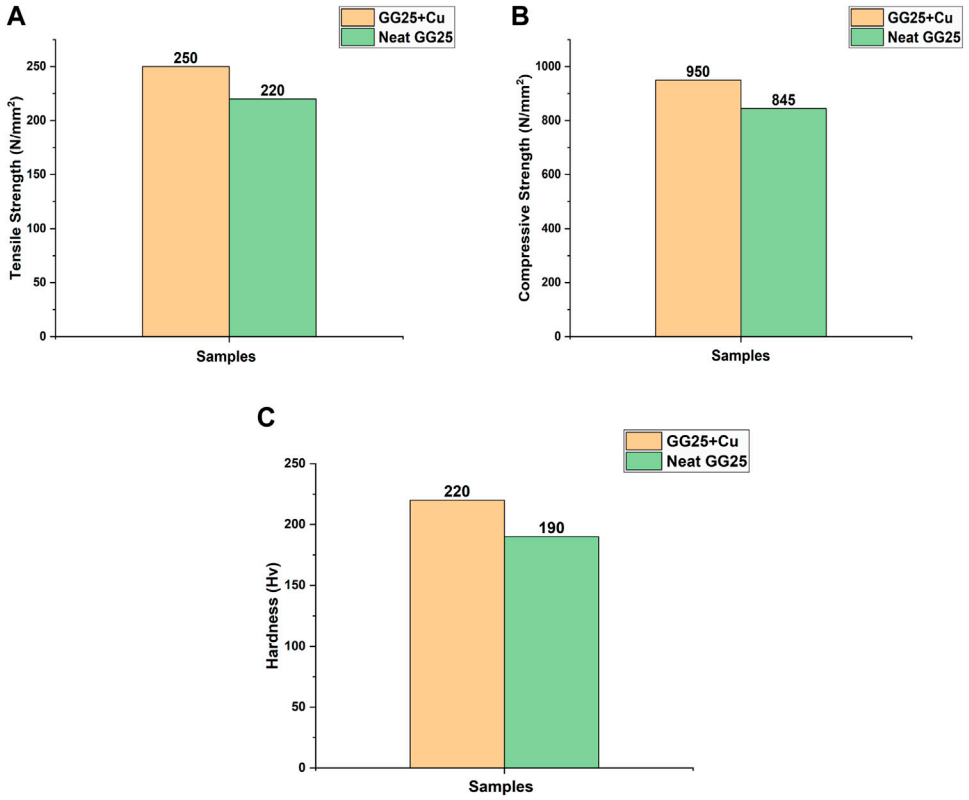

FIGURE 3
(A). Tensile Strength, **(B)**. Compressive Strength, and **(C)**. Hardness of GG25+Cu and GG25 samples.

TABLE 3 Mechanical Properties of GG25+Cu and GG25 sample.

Mechanical property	GG25 + Cu	GG25 only
Porosity	0.8%–1%	–
Tensile Strength	250 N/mm^2	220 N/mm^2
Compressive Strength	950 N/mm^2	845 N/mm^2
Hardness	220 Hv	190 Hv

micron diamond paste. The specimen is made in accordance with E3-11 (2017) standards.

The Nital solution (100 mL of ethanol +10 mL of nitric acid) was used for etching. After that, the specimen was observed at 1,000x magnification with an inverted optical microscope. Figure 4 displays the microstructure that was observed.

Copper promotes pearlite structure and with the addition of copper, the volume of graphite decreases. With increasing copper content, a fine pearlite structure is observed.

3.4 XRD analysis of cast sample

The XRD analysis for cast samples GG25 is represented in Figure 5. Iron exists in the matrix as alpha iron as evident from X-ray peaks. Also, α-Fe with little Si solid solution is also formed i.e., ($Fe_{19}Si$) 0.1. Carbon exists in the form of graphite flakes or nodules depending upon the content of silicon in the matrix (Ranakoti et al., 2022). It is due to this graphite film that aids lubricating action and helps to minimize wear loss. Silicon also increases the grain size (Cui et al., 2022). It also helps in increasing the length of the graphite flakes. Hardness is however decreased due to Si addition in the CI matrix.

On the other hand, Mn produces hard carbides within the microstructure. This improves the hardness as well as the toughness of the cast samples (Yadav et al., 2023). A mix of ferritic film along with the lubricating film protects the wear loss of the cast iron samples. Mn and sulphur combine to form manganese sulphides, and MnS also acts as a solid lubricant. It also contributes to the machinability of the cast iron samples (Singh et al., 2022). Structural graphite and the inherent lubricating tendency of MnS always tend to minimize the co-efficient of friction between the pin and the disc surface.

3.5 XRD analysis of worn out sample

After the conduct of wear tests under dry sliding conditions, the surface of GG25 +Cu samples showed the presence of wear tracks and plastic deformations. The surface debris was collected and XRD analysis revealed that the brown particles are iron oxide (Fe_3O_4) particles that originated during direct metal-to-metal contact during the conduct of wear tests. This is also evident in the XRD analysis as shown in Figure 6.

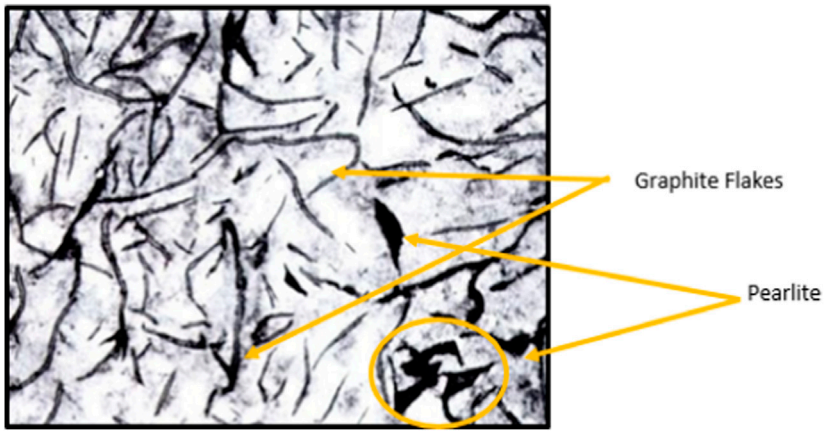

FIGURE 4
Metallographic analysis of GG25 +Cu Sample.

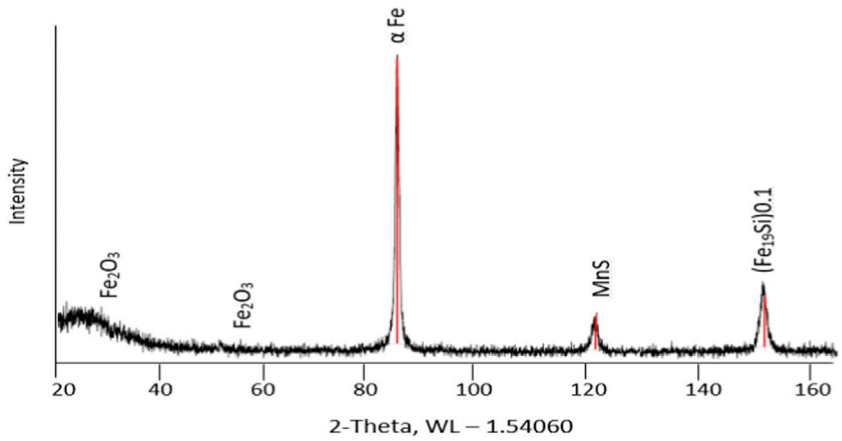

FIGURE 5
XRD pattern of cast sample.

3.6 Effect of varying load at a constant velocity on wear

The effect of increasing constant load on the wear, and coefficient of friction has been shown in Figures 7A–F respectively.

At 30N of load, at the onset of the wear cycle; wear loss increases rapidly for 250 m sliding distance and then further increases to almost double the rate at 600 m sliding distance. It has been reported that maximum wear occurs during this sliding interval and a lot of material loss takes place due to lose particles which further increases the wear rate due to three body abrasion wear mechanism (Rajawat et al., 2022). It has been reported that wear values reduce to 1/7th of wear value after 600 m sliding distance in comparison to wear losses during the running-in period. The continuous formation of the graphitic film occurs till the end of the wear cycle i.e., 5400 m sliding distance. Also, fluctuations in the wear measurement occur at 1250 m and 1800 m sliding distances due to uneven formation of the protective graphitic film. To avoid this, care should be taken to clean the wear tracks at defined time intervals.

At 40N, due to a high normal load, at the very onset of the cycle wear loss is suffered but a graphitic layer is soon developed which protects the sample pin from further wear loss. Also, the temperature at the interface becomes high and results in a smearing action of the graphite layer at the interface (Singh et al., 2021b; Ganeshkumar et al., 2022; Li et al., 2022). Graphite layers are weakly bonded to each other. Higher loads result in higher friction. Due to this, the temperature rises and these weakly bonded graphite layers shear and transfer to the mating components. An increase in friction due to increasing loads results in higher temperatures and this further actuates the smearing action of the graphite layers at the interfaces of the mating components. As the investigation provides a comprehensive analysis of the temperature sensitivity of the graphite layer and its influence on wear behaviour. This also minimizes the direct contact between pin samples and the hardened disc (Kumar et al., 2020; Cui et al., 2023; Miniappan et al., 2023).

In addition, the current study has aimed to examine the wear characteristics of cast iron GG25 specimens with copper additions, while subjecting them to various loads and sliding speeds. The

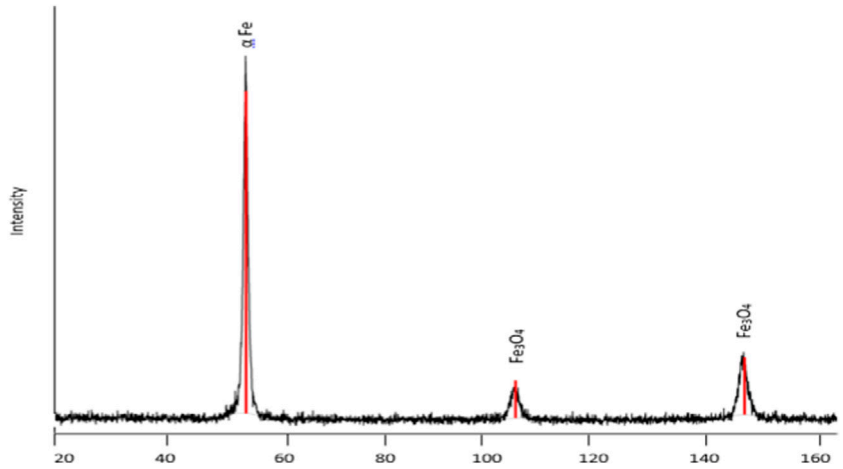

FIGURE 6
XRD pattern of cast sample.

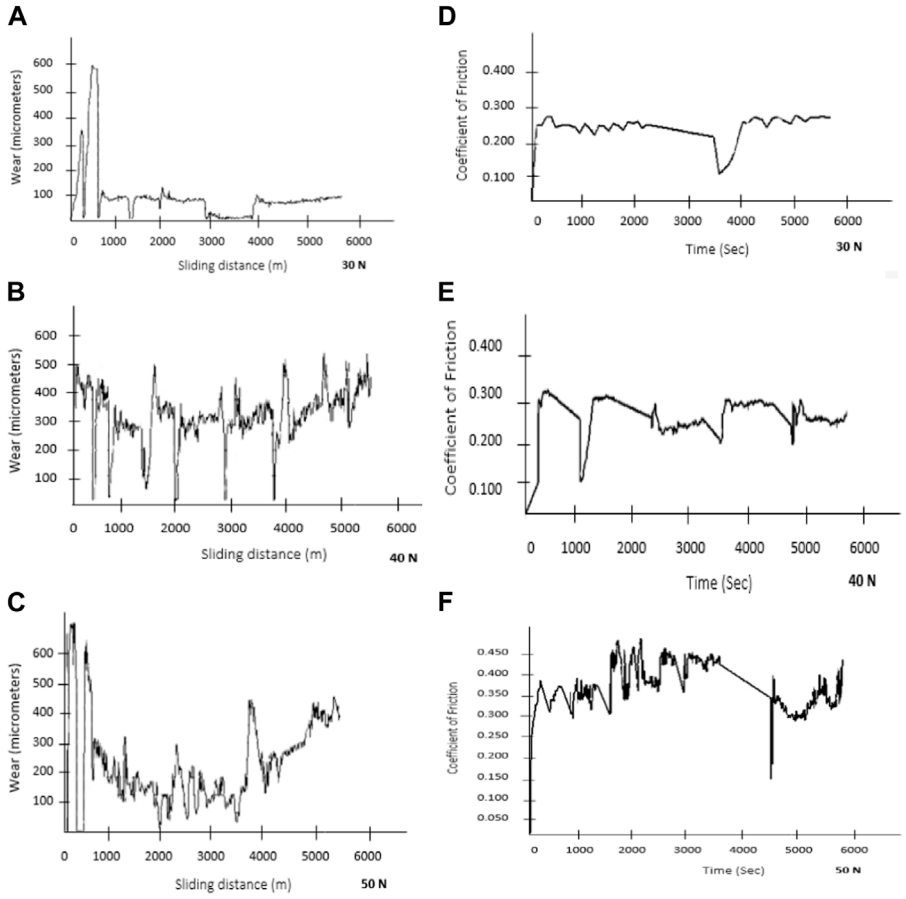

FIGURE 7
Effect of varying load (30,40 &50 N) at constant velocity 1 m/s on wear **(A–C)** and Coefficient of friction **(D–F)**.

inclusion of graphite inside the cast iron matrix plays a pivotal role in mitigating the adverse impacts of wear. Under higher loads, the temperature at the contact-interface exhibits a rise, leading to the phenomenon of matrix softening (Jia et al., 2022; Liu et al., 2023a; Liu et al., 2023b). The process of softening reduces the bonding strength between graphite particles and the matrix in the mechanical

contact-interface. During the occurrence of sliding wear, the application of normal and tangential stresses culminates in the occurrence of plastic shear deformation on the surface that is comparatively softer (Cheng et al., 2021; Lashin et al., 2022; Wang et al., 2022). This deformation leads to the initiation of cracks and the production of debris in the form of flakes. This particular process is commonly referred to as delamination (Sehar et al., 2022; Dikshit et al., 2023).

At lower applied loads, namely, 30N, the occurrence of adhesive wear tracks and the presence of loose debris originating from the cast iron matrix are factors that contribute to the overall wear losses. When subjected to a load of 40N, the sample undergoes a phenomenon wherein a graphitic layer forms, serving as a protective barrier against further wear. Additionally, the rise in temperature at the interface facilitates the smearing action of the graphite layer (Shahid et al., 2022; Kumar et al., 2023c; Singh et al., 2023). The occurrence of this smearing phenomenon may be ascribed to the shearing and transfer of weakly bound graphite layers onto the mating components. This process serves to minimise direct contact between the pin samples and the hardened disc (Kiranakumar et al., 2022; Kumar et al., 2023d; Prasanthi et al., 2023).

Nevertheless, when subjected to the maximum stress of 50N, sub-surface fractures/crevices or cracks emerge among the graphite flakes discovered within the wear surface, hence signifying the occurrence of substantial wear (Liao et al., 2020; Niu et al., 2022; Vemanaboina et al., 2023). The aforementioned data indicate that the smearing action of the graphite layer at the interface is subject to the impact of the applied loads. Raised loads lead to higher temperatures and enhanced smearing action, hence facilitating the reduction of direct contact and mitigating wear losses (Fu et al., 2020; Guo et al., 2022; Niu et al., 2022).

Moreover, when subjected to various sliding velocities, the inclusion of graphite particles functions as a solid lubricant. At lower velocities, namely, at 0.5 m/s, the presence of detached particles or loose-debris becomes apparent as a result of the contact-load, hence leading to an immediate rise in wear (Zhu et al., 2017; Zhu et al., 2021). Nevertheless, the development of an oxide layer and the process of work hardening in metallic particles serve as effective mechanisms in mitigating further wear. At velocities considered moderate, namely, 1 m/s, loose particles and the presence of an oxide layer serve as protective measures, effectively mitigating the occurrence of significant wear on the samples. Insufficient presence of solid lubricant at high velocities, namely, at a rate of 2 m/s, imparts rise to the development of fissures/cracks/fractures/ruptures/holes/craters within the graphite layer, thus leading to significant wear (Yu et al., 2023a; Zhao et al., 2023).

All in all, the phenomenon of smearing occurring at the interface of the graphite layer is intricately related to the magnitude of the applied-load and the velocity at which sliding occurs. Higher loads and moderate sliding velocities provide efficient smearing, resulting in reduced direct contact and lowered wear losses (Shi et al., 2023a; Xu et al., 2023). The influence of graphite and its response to numerous conditions are of substantial significance in determining the wear resistance characteristics of cast iron GG25 samples incorporating copper reinforcements (Liu et al., 2020; Shen et al., 2022).

Now, from the Formation of Graphite and Its Significance point of view, the matrix of cast iron is characterised by the presence of graphite particles dispersed throughout (Liu et al., 2023c). Graphite functions as a solid lubricant, effectively mitigating friction and minimising surface wear in sliding systems (Bai et al., 2023; Shi et al., 2023b).

The findings of the study suggest that the inclusion of copper serves to enhance the refinement of graphite flakes, hence facilitating the development of an additional finer pearlite matrix (Yu et al., 2023b). This refinement leads to enhancements in the mechanical characteristics, namely, in terms of wear resistance and hardness (Hu et al., 2023; Wu et al., 2023).

The process of graphite coarsening and stabilisation is facilitated by the presence of copper, resulting in enhanced wear resistance (Li et al., 2023). Additionally, copper has the effect of minimising the coefficient of friction between the pin and the surface of the disc (Liu et al., 2023d).

In accordance with the temperature dependence of Graphite Sensitivity, at higher temperatures experienced during the process of sliding wear, the graphite layer experiences numerous changes.

At low temperatures, namely, within the range of room temperature to moderate levels, graphite demonstrates its efficacy as a solid lubricant by effectively avoiding direct contact between metal surfaces. This characteristic serves to mitigate wear and friction, hence enhancing the overall performance and durability (Güneş et al., 2021a).

The phenomenon of weakly bound graphite layers shearing and transferring to mating components, therefore functioning as a lubricating film, is observed with the rise in temperature from moderate to high values (Usca et al., 2021). Nevertheless, under exceptionally high temperatures, it is plausible for the graphite layers to undergo degradation, hence resulting in escalated rates of wear.

The phenomenon of graphite oxidation occurs when graphite is exposed to oxygen during wear testing, resulting in the formation of iron oxides. This chemical reaction has the potential to impact the wear behaviour of the material (Güneş et al., 2021b). The detection of iron oxide (Fe_3O_4) particles serves as an indication of the occurrence of oxidation in wear testing.

In context with the influence of load and sliding velocity, the phenomenon of load variation results in elevated temperatures at the interface, leading to a reduction in the hardness of the matrix material. The process of softening reduces the bonding strength between graphite particles and the matrix, which causes raised rates of wear (Korkmaz et al., 2023).

The phenomenon of sliding speed is characterised by the presence of loose debris and work-hardened surface particles, which function as a solid lubricant and effectively reduce the occurrence of wear at lower speeds. At rising velocities, the quantity of graphite diminishes as a result of compression, resulting in the development of fractures and heightened abrasion.

Moreover, the application of "Energy Dispersive X-ray Spectroscopy (EDX)" has provided confirmation about the existence of carbon and its different forms in both the as-cast and worn-out samples. The higher carbon concentration is indicative of a raised graphite content, hence implying enhanced wear resistance of the material (Korkmaz et al., 2023).

The presence of oxygen in deteriorated samples suggests that oxidation has occurred as a result of exposure to oxygen in the atmosphere during the process of wear testing.

In essence, the presence of a graphite layer within cast iron GG25 is of paramount significance in enhancing its resistance to wear under dry sliding conditions, as it functions as a solid lubricant. The behaviour of the same has exhibited sensitivity to variations in temperature, load, and sliding velocity. The incorporation of copper into the graphite structure results in the refinement of its microstructure, thus enhancing its resistance to wear. The presence of oxygen during wear testing has the potential to induce oxidation, hence impacting the material's wear characteristics.

Furthermore, the investigation indicates that there is a significant rise in wear rate when subjected to higher loads (40N and 50N) and sliding speeds (1 m/s and 2 m/s). The observed escalation in the rate of wear can be attributed to the elevated temperature occurring at the interface. When the applied loads are enhanced, there is an accompanying rise in the frictional forces experienced by the mating components, resulting in a subsequent rise in temperature.

The phenomenon of graphite smearing is elucidated in the text, wherein it is said that when a normal load of 40N is applied, the temperature at the contact rises, leading to the occurrence of smearing of the graphite layer at said interface. The layers of graphite, which serve as a source of lubrication, have a relatively lower extent degree or level of bonding strength. The application of high loads and temperatures induces the shearing of poorly bound graphite layers, leading to their transfer onto the mating components. The use of graphite layers serves to mitigate direct contact between the pin samples and the hardened disc.

The wear rate appears to rise at higher sliding speeds (2 m/s) as a result of the inadequate smearing of the graphite and oxide layers, hence underlining the impact of sliding speed. The lubrication mechanism has been harmed, leading to a substantial rise in the rate of wear. This observation suggests that the rise in temperature resulting from higher sliding velocities additionally enhances the smearing mechanism and wear.

The examination of the deteriorated sample, as detected using SEM imaging, offers visible confirmation of the occurrence of smearing, fractures, and deformation within the graphite layers resulting from rising temperatures and applied loads.

Furthermore, the raised temperature observed at the interface between the pin and the hardened disc during wear testing can be attributed to the frictional forces generated among the sliding surfaces. The raised temperature contributes to the smearing phenomenon of the graphite layer at the interface. The process unfolds as follows:

The phenomenon of high load and smearing action occurs when the magnitude of the applied load is increased leading to a corresponding rise in the contact pressure between the pin and the disc. The increased pressure leads to an enormous rise in frictional heat at the interface-point. The graphite layers present in cast iron, which exhibit a lubricating property, are characterised by a relatively weak interlayer bonding. Under conditions of higher temperature and pressure, the graphite layers that are held together by weak bonds undergo shearing and transfer onto the adjacent mating-components. The aforementioned occurrence is commonly denoted as smearing.

The inclusion of graphite within the cast iron matrix serves as a solid lubricant. In usual situations, the presence of a lubricating coating serves to mitigate direct contact between the pin and the disc, hence diminishing friction and minimising wear. Nevertheless, when subjected to higher loads and temperatures, the graphite layers have the potential to undergo shearing and subsequently migrate to the adjacent mating-components, therefore facilitating the lubricating of the interface.

The formation of a protective coating occurs when the sliding surfaces experience low loads and speeds, leading to the development of graphite layers that effectively mitigate wear. Nevertheless, when subjected to higher loads and velocities, the protective coating may experience breakdown, degradation, or shear-off due to the considerable amounts of friction and heat (Korkmaz et al., 2023). The aforementioned disintegration reveals fresh graphite, which subsequently has the ability to smear over the contacting mating-surfaces, thus offering transient momentary lubrication until it eventually diminishes.

The first reduction in wear is attributed to the smearing effect of graphite layers. Nevertheless, in conditions of excessive loads or velocities, the lubrication mechanism may become inadequate, leading to higher rates of wear over prolonged sliding distances (Korkmaz et al., 2023).

Additionally, the raised temperature at the interface plays a critical role in facilitating the smearing action of the graphite layer, hence influencing the material's wear characteristics. Now, the analysis and the rationales with thorough evidence underlying this phenomenon have been elucidated as follows.

i. **The phenomenon of rising temperatures occurring at the interface:** Frictional heating occurs when two materials undergo relative motion, such as in the pin-on-disc test done within the context of the present investigation. The interaction between the materials during this process results in the generation of thermal energy (Korkmaz et al., 2023). The thermal energy is localised at the boundary between the surfaces undergoing sliding motion. At higher loads and velocities, the contact pressure intensifies and the relative motion between the materials accelerates. The heightened pressure and motion result in the generation of additional frictional forces, hence causing a rise in temperatures at the contact interface (Korkmaz et al., 2023).
ii. **The phenomenon of smearing caused by the graphite layer:** The inclusion of graphite in cast iron serves as a solid lubricant (Korkmaz et al., 2023). The self-lubricating characteristics of graphite can be attributed to its layered structure, which facilitates efficient shearing.
iii. **The Impact of Elevated Temperatures:** The rise in temperature causes a reduction in the hardness of the graphite and the surrounding material at the contact interface. The phenomenon of softening arises due to the reduction in mechanical strength demonstrated by materials when exposed to higher temperatures, rendering them particularly vulnerable to deformation (Korkmaz et al., 2023).
iv. **The phenomenon of shearing graphite layers:** The higher temperature causes the occurrence of shearing in the graphite layers that are held together by weak bonds. The application of shear force induces the graphite layers to undergo smearing and

then adhere to the adjacent components, namely, the hardened disc in this particular scenario. Smearing refers to the phenomenon in which graphite material diffuses and sticks to the surfaces in contact, resulting in the formation of a protective layer (Korkmaz et al., 2023).

v. **The Influence on Wear Behaviour:** The application of graphite leads to the formation of a protective coating on the surfaces of the mating components. The primary function of this film is to serve as a lubricant, effectively minimising the extent of direct contact between the pin and the disc (Korkmaz et al., 2023). Consequently, it serves to reduce both wear and friction between the materials.

The study demonstrates that the wear rate is subject to variation as a result of the applied load and sliding speed. Under higher stresses, the wear rate experiences an initial rise as a consequence of fracture development and subsequent rupture of the protective graphite film. At higher velocities, the effectiveness of the graphite and oxide layers in maintaining their integrity at the contacting surface interfaces diminishes, resulting in higher rates of wear (Korkmaz et al., 2023).

In summary, the raised temperature occurring at the contact interface induces a state of softening in the graphite layers within the cast iron samples. The process of softening, in combination with the heightened stress and velocity, enables the graphite layers to be smeared over the mating components by a smearing motion. The application of smeared graphite results in the formation of a protective coating, which serves to mitigate direct contact and hence minimise the occurrence of wear. Nevertheless, in conditions of excessive loads or velocities, the integrity of the protective film may deteriorate, resulting in accelerated rates of wear.

All in all, the raised temperature experienced at the contact interface induces a softening effect on the matrix material, thereby diminishing the mechanical bonding strength among the graphite particles and the matrix. The lubricating effect of graphite layers, while initially advantageous in reducing direct metal-to-metal contact, may become undermined under severe circumstances, resulting in wear and material degradation (Korkmaz et al., 2023).

At 50N of normal load, the wear rate is very high for the initial 100 m of sliding distance. This happens due to the formation of the cracks during the running cycle. These further rupture the protective film. After 500 m of sliding distance, the wear rate starts decreasing and continues till 3,500 m of sliding distance. After this, the wear rate again starts increasing because the graphitic film is diminished and unable to be retained due to the high normal load. The wear rate continues to increase again till the end of the wear cycle.

3.7 Effect of varying sliding velocity at constant load on wear

The influence of raising the sliding velocity at 0.5, 1, and 2 m/s has been shown on the wear, and coefficient of friction at 30 N constant load in Figures 8A–F respectively. At 0.5 m/s, the sliding speed is slow but the loose particles are released due to the contact load of 30 N. These loose debris are responsible for increased wear. After 1000 m of sliding distance, an oxide layer is formed. This partial oxide film along with graphitic film on the wear track minimizes the wear loss and the material suffered the least wear loss till the end of the cycle. On increasing the sliding speed up to 1 m/s, the loose debris are released during the running in period i.e., 600 m sliding distance. These loose particles along with the oxide layer prevent further wear loss. Due to increased speeds, these loose particles are work hardened, and subsequent oxidation of metallic particles also takes place. This shiny layer formation prevents any further wear till the end of the cycle. At sliding speeds of 2 m/s, up to 2000 m sliding distance, wear rate considerably increases. This occurs due to the unavailability of solid lubricant to be smeared effectively and interrupts the formation of lubricating film on the contacting surfaces. After 2000 m, cracks appear in the graphite film and the de-cohesion results in severe wear. At high speeds supply of graphite decreases as a result of the compression of the graphite flakes, and results in the formation of crack-like features. This is further evident after 4000 m, wear continues to increase many folds due to in efficiency of the graphite and oxide layers to sustain at the mating surfaces. Lubricating action is compromised and maximum wear is encountered by the samples.

3.8 Cumulative weight loss (gms.) of different samples under varying loads and sliding speeds

As shown in Table 4, this increase in the weight loss values for the GG25 cast samples at higher applied normal load is due to the higher temperature at the interface. This increase in the temperature at the interface causes the softening of the matrix, which results in weakness in mechanical interface bonding strength between graphite particles and the matrix.

Another concept behind this is that the normal and tangential forces introduced during sliding wear will induce plastic shear deformation of the softer surface. Continued subsurface deformation will ultimately cause crack nucleation below the surface (but not very near the surface). These cracks join due to crack propagation and take the form of the 'delaminate', giving rise to the generation of flake-type debris.

It has been noted that up to medium sliding speed (0.5 m/s to 1 m/s), with the increase in sliding speed, weight loss increased at room as well as higher temperature. This is because of the solid lubrication effect of the graphite particles which are not being removed from the contact area and safeguards the cast samples.

3.9 Wear rate

Figures 9A–F wear graph makes it clear that as the constant load is raised from 30 N to 50 N, wear loss rapidly increases. However, the wear rate significantly increases from 0.5 m/s to 2 m/s, showing considerable wear loss at higher speeds. While it stays constant as sliding speeds increase, the friction coefficient also rises with increasing constant loads. When conditions change from low to moderate, frictional forces first rise, then fall when conditions change from moderate to higher. This occurs as a result of loose debris and work-hardened surface debris at the sliding disc and pin interface (Ganeshkumar et al., 2022). The CoF values are mean values and the standard deviation ranges from 0.026 at min to 0.030 maximum for all 5 samples.

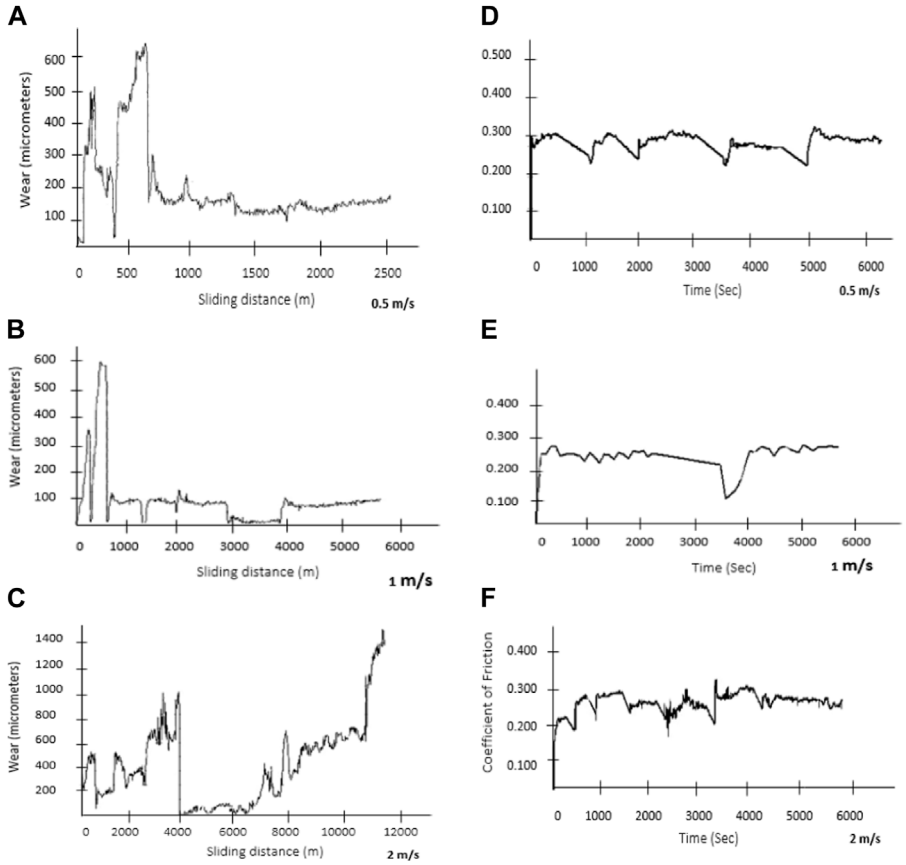

FIGURE 8
Effect of varying sliding velocity (0.5, 1, and 2 m/s) at a constant load of 30N on wear **(A–C)**, and Coefficient of friction **(D–F)**.

TABLE 4 Cumulative Wear loss for Cast Iron GG25 sample at Room Temperature.

Cumulative weight loss (gm)					
Time (mins)	Sample 1	Sample 2	Sample 3	Sample 4	Sample 5
5	0.032	0.002	0.009	0.005	0.006
10	0.035	0.007	0.014	0.009	0.02
20	0.036	0.016	0.028	0.024	0.042
30	0.04	0.026	0.034	0.039	0.066
45	0.041	0.034	0.051	0.064	0.083
60	0.045	0.05	0.068	0.089	0.106
90	0.054	0.084	0.101	0.129	0.141

3.10 Worn out samples analysis

Figures 10A–F, exhibits the wear mechanisms as observed in the worn cast iron samples during the experimental runs. The cast iron GG25 belongs to the pearlite phase family. Lamellar structure and its composition affect the wear behavior. Pearlite phase exhibits the phenomenon of deformation strengthening which contributes to the wear resistance of the alloy (Li et al., 2022). However, with the addition of 2.4% copper, GG25 also develops a fine pearlite phase.

At normal loads of 30N, adhesive wear tracks appear at the pin and disc sliding interface. These are brittle in nature and are released as loose debris from the cast iron matrix. On further increasing the load to 40N, these loose particles along with deformed graphite layers contribute to wear losses. It has been concluded that abrasive wear which is generally accompanied by delamination is initiated due to lose particles. At 50N of normal load, sub-surface cracks are developed at the suitably oriented graphite flakes within

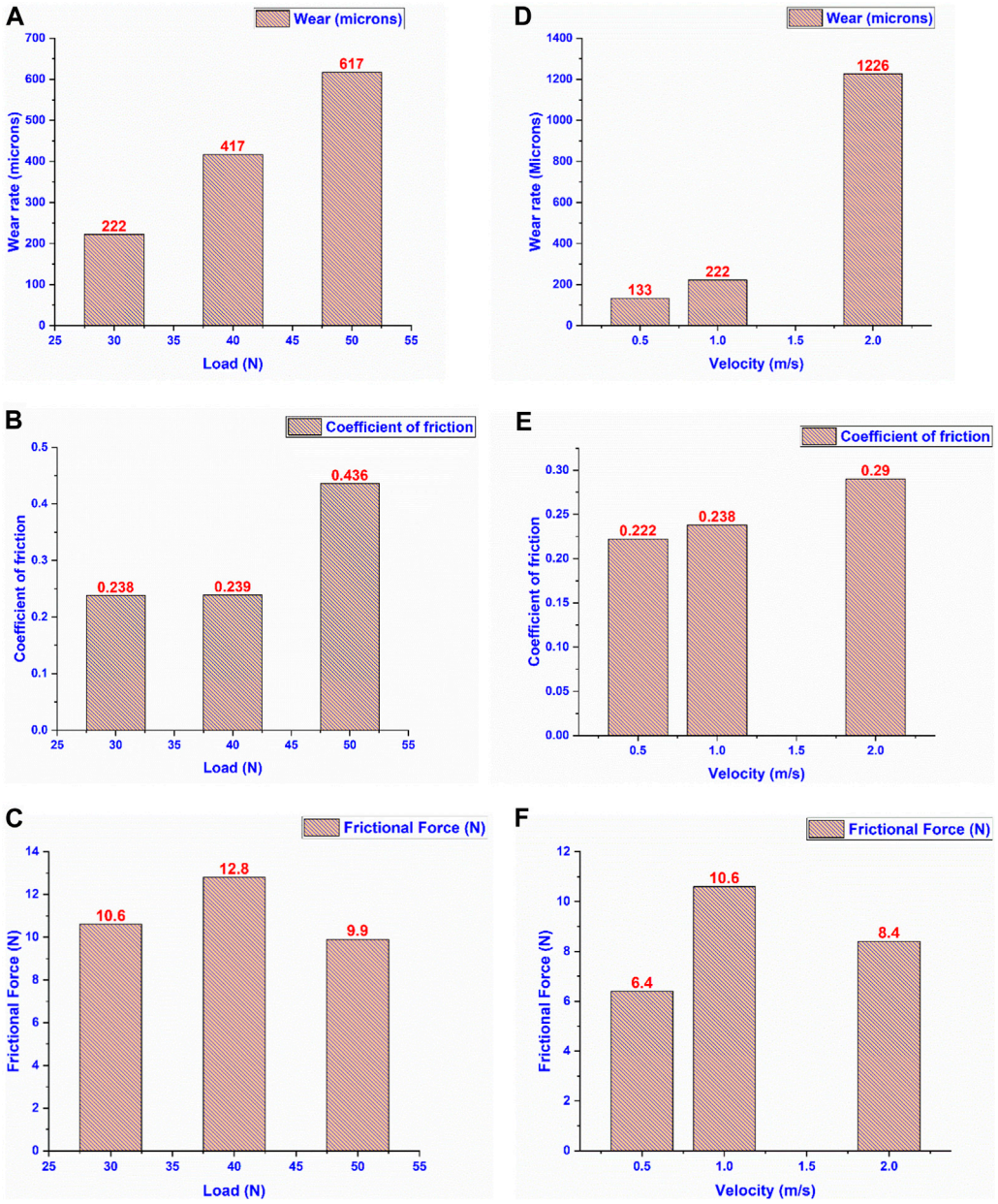

FIGURE 9
(A–F). Wear rate, CoF, and frictional force with varying loads **(A–C)** and varying sliding speeds **(D–F)**.

the un-deformed cast iron matrix beneath the wear surface (Liu et al., 2023a).

At the low sliding speed of 0.5 m/s, and low load of 30N, the polished surface appearance indicates the formation of graphite film and the sample exhibits minimum wear loss and minimum friction coefficient. At increased speeds of 1 m/s, graphite film and partial oxidation of loose wear particles protect the samples from severe wear losses. The smearing of graphite film and subsequent oxidation of metallic fragments are observed at this stage. These metallic fragments are work hardened at higher speeds of 2 m/s. The work hardening is due to three body abrasion and results in the formation of pits and ploughs as evident in the SEM micrographs.

3.11 EDX analysis of as cast and worn out GG25 + Cu sample

3.11.1 EDX of as-casted sample

Following surface morphology analysis on GG25 samples that have been cast. Further, Energy Dispersive Spectroscopy is used to do the compositional analysis (EDS). Figure 11 shows that the highest level of carbon was discovered to be present following iron. Carbon is present up to 20.3% in the spectrum 2, as can be shown. A higher carbon content in the matrix of the cast iron suggests a higher graphite content (Wang et al., 2022). This graphite content exists as flakes and tends to prevent surface wear on the samples during the conduct of wear tests.

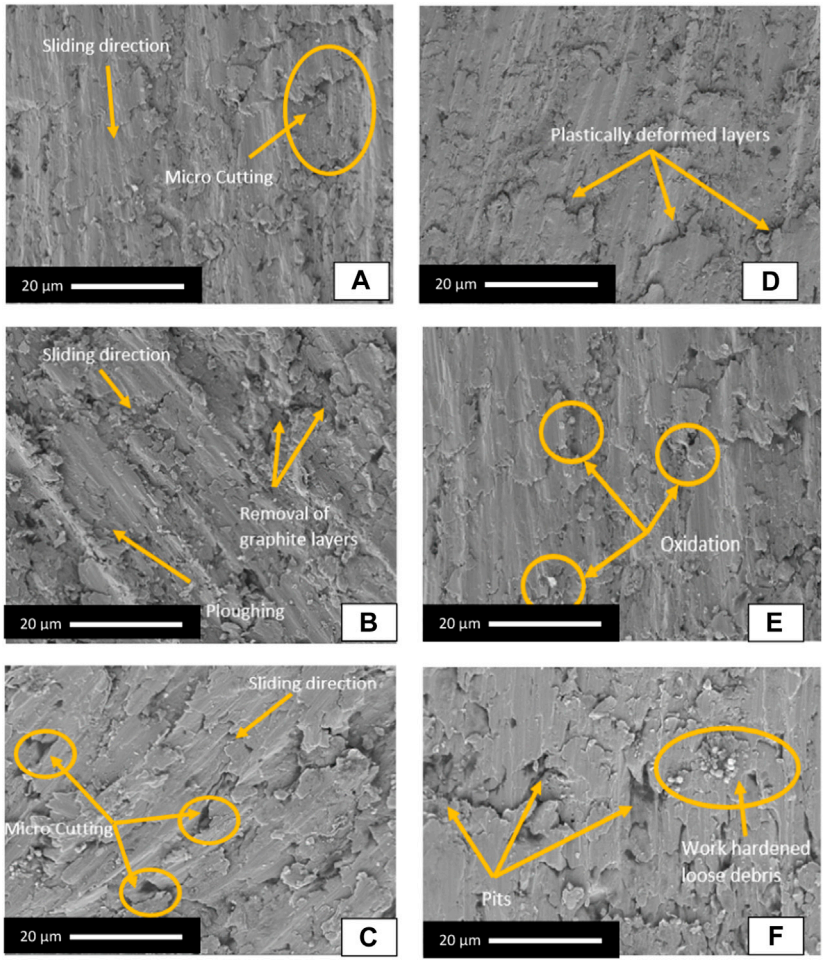

FIGURE 10
(A–F). Worn out samples analysis at varying loads **(A–C)** and varying velocities **(D–F)**.

3.11.2 EDX of worn-out sample

In Figure 12, it is shown that along with iron, a high presence of carbon has been observed. The higher percentage of carbon indicates a higher percentage of graphite in the cast iron matrix. As seen in the spectrum 13, 14, and 15, the percentage of carbon was 22.8, 23.5, and 29.7%, respectively. During the wear testing, the sample pin is exposed to atmospheric oxygen and is prone to oxidation. This is evident because of shiny metallic debris as well. In the spectrum 13, 14, and 15, the percentage of oxygen is 1.5, 1.4, and 2.1% respectively. Silicon increases the grain size and the length of graphite flakes. This ultimately decreases the hardness of the matrix. In the spectrum, Si is 0.9, 1.1, and 0.8% respectively (Dikshit et al., 2023).

4 Conclusion

GG25 valve materials have improved wear characteristics, longevity, self-lubricating, thermally stable, etc. Due to the introduction of positive seals in the cylinder head, valves, and valve guides are deprived of proper lubrication. In the absence of lubrication wear increases and frictional losses increases. This results in higher fuel consumption and decreases the life of the engine components due to embrittlement. It is shown that cast iron with suitable alloy compositions can significantly improve the life and wear performance of the components. Since the valve guides operate in dry conditions, experimental results showed that Cast iron GG25 + 2.40% Cu is a better choice for the selection of valve guide material.

The findings of the wear studies indicate that normal load exerts an additional substantial influence under moderate loading and speed conditions. However, as the sliding velocity rises, the role of the normal load becomes more significant, culminating in higher wear losses. Additionally, frictional forces and the coefficient of friction have been determined and were discovered to rise as the loading increased. Using SEM analysis in conjunction with EDX analysis, the wear mechanisms were explored. The outcomes revealed that a rise in sliding speed contributed to significantly higher wear losses in comparison to raised loading conditions. The GG25 grade of cast iron employed in this investigation comprises a minimal amount of copper and phosphorus content. The interstitial strengthening mechanism has been reported to have an implication on mechanical characteristics, including strength and hardness. Furthermore, the incorporation of

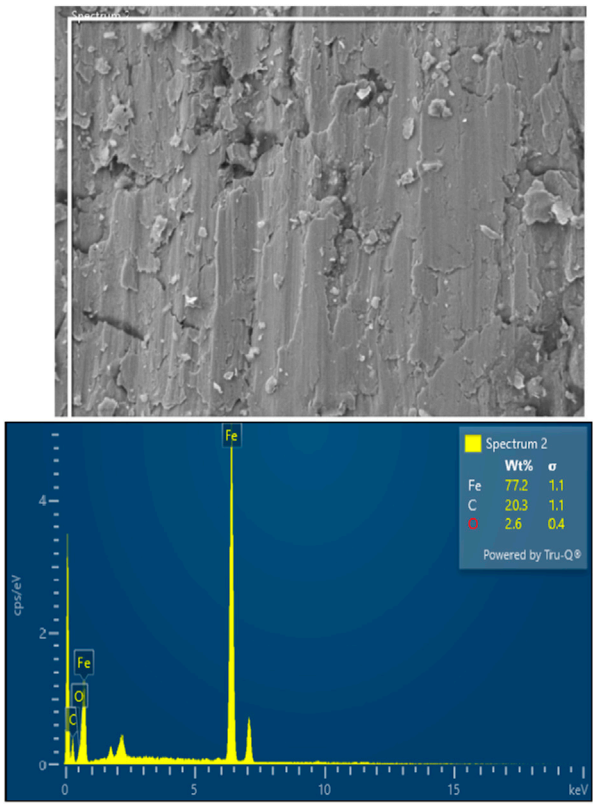

FIGURE 11
Compositional analysis of as Cast GG25 + Cu sample.

copper facilitated the development of a fine pearlite matrix, which served to enhance both wear resistance and hardness. With a rise in copper content, metallographic analysis revealed the presence of pearlite structures and a reduction in graphite volume. The analysis of worn-out and cast samples employing XRD analysis yielded valuable information regarding the chemical-composition of the matrix, the formation of graphite-films, and the lubricating characteristics of different elements present in the cast iron.

Additionally, the impact of varying loading and sliding velocities on wear characteristics was investigated. This observation underscored the significance of graphite as a solid lubricant, which effectively reduced wear at moderate speeds as well as lower loads but posed difficulties at higher speeds. The research placed significant emphasis on the implications of temperature, load, and sliding velocity on wear-rates and the lubricating graphite layer's efficiency or functionality efficacy. In addition, an analysis for cumulative weight loss revealed that higher applied normal loads resulted in higher weight loss owing to higher temperatures, which induced matrix deformation. It was discovered that the rate of wear escalated as the constant loads and sliding velocities increased. Additionally, the wear mechanisms of worn-out samples differ with regard to the load and sliding speed conditions. The element-composition characteristics of as-cast, as well as worn-out samples, were determined using EDX analysis, wherein higher carbon contents inferred a rise in the amount of graphite present in the cast iron matrix. The research outcomes indicate that the inclusion of a graphite layer substantially enhances the resistance to wear, which is sensitive to variations in temperature, load, as well as sliding velocity.

The research is centred on GG25 cast iron that has been reinforced with copper via sand casting and induction furnace techniques. The incorporation of copper enhances mechanical characteristics such as

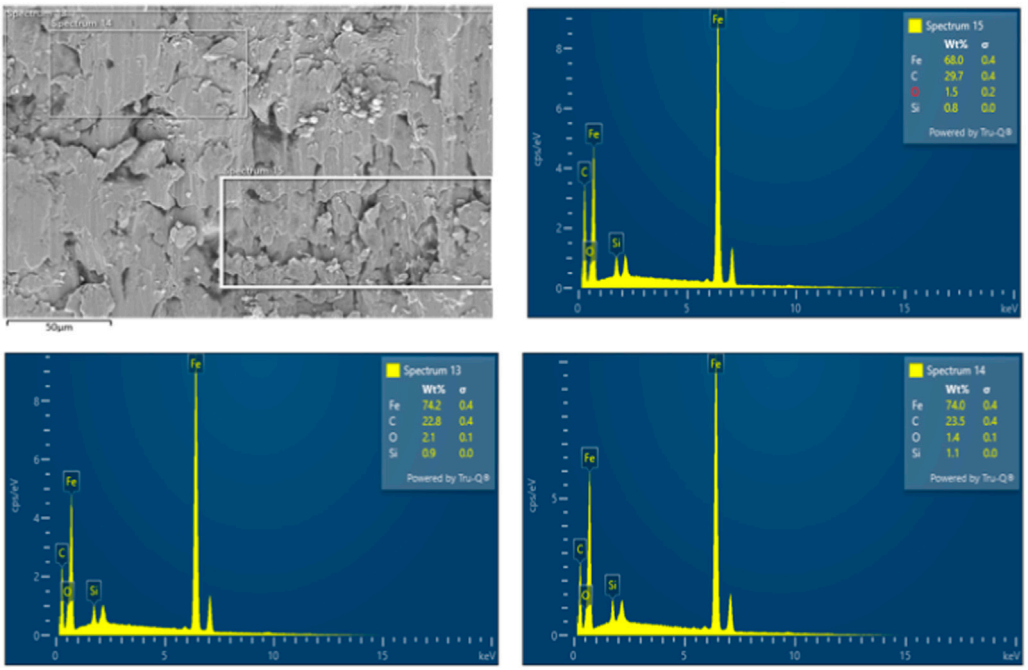

FIGURE 12
EDX of worn-out samples.

strength and hardness, by promoting the development of a fine pearlite matrix and reducing the size of graphite flakes. XRD and metallographic analyses validate the microstructural variations that copper inclusion induces, which contributes to enhanced resistance to wear. Iron oxide particles (Fe_3O_4) are identified by XRD analysis of worn samples, which can be ascribed to the direct metal-to-metal contact that occurs during wear studies. Additional research is conducted to determine how varying loads and sliding speeds impact wear behaviour. Under various conditions, the incorporation of graphite into the cast iron matrix functions as a solid lubricant, thereby impacting the resistance to wear. Rising temperatures at the interface of contact, which are caused by higher loads and sliding velocities, have an enormous implication on the behaviour of wear. According to the findings of the investigation, the incorporation of copper into graphite particles enhances their hardness and resistance to wear. The wear characteristics of graphite layers exhibit differences in response to variations in temperature, load, and sliding velocity, thereby emphasising their temperature sensitivity. The study offers an in-depth investigation of the wear mechanisms, the phenomenon of graphite smearing, and the implications of copper on the wear characteristics of GG25 cast iron.

All in all, the experimental trials have been conducted at low as well as high normal loads and sliding speeds to simulate the real conditions. Combined, the addition of copper and limiting phosphorus improves the life span of the components with improved mechanical properties. The following inferences can be deduced based on experimental runs.

i. Copper promotes the formation of pearlite in cast iron and improves the material's tensile strength and toughness.
ii. The formation of a fine pearlite matrix imparts high hardness and thus improves compressive strength.
iii. Graphitization is accelerated by the addition of Cu, but the size of the graphite flakes also decreases.
iv. Alloying element copper tends to delay nucleation and the growth of the graphite flakes. Hence, in the present study, Cu is limited to 2.4%.
v. At a low sliding speed of 0.5 m/s and constant load of 30 N, a minimum wear loss of 133 microns is observed as graphite smears at the interface and thus prevents metal-to-metal contact.
vi. At a higher speed of 2 m/s and constant load of 30 N, maximum wear of 1,226 microns is observed because higher speeds induce higher friction. Higher friction further increases the temperature and shear forces at the interface. The reduction of the oxide layer also takes place and contributes to maximum wear loss.
vii. At a low load of 30 N and constant sliding speed of 1 m/s, wear loss is 222 microns which almost doubles i.e., 417 microns on increasing the load at 40 N due to contact metal asperities.
viii. At a high load of 50N, cracks develop. This happens because graphite flakes leave behind crack-like features in the cast iron matrix. These cracks tend to propagate and enhance wear rates.
ix. The formation of the oxide layer formation Fe_2O_3 acts as a protective film and prevents direct metal-to-metal contact. At higher temperatures, the oxide films are reduced and the wear loss increases.
x. A metastable solid solution of α-Fe with silicon i.e., ($Fe_{19}Si$) 0.1 promotes the formation of soft graphite flakes and thus minimizes the wear.
xi. The examination of worn-out cast samples revealed that micro-cutting, Ploughing, and delamination were the main wear mechanisms.

In summary, this extensive investigation offers significant knowledge regarding the dry sliding characteristics of cast iron GG25 when copper is incorporated. It illuminates the complex connection among various factors that impact the resistance to wear for valve guide applications. The findings of this study enhance comprehension regarding the behaviour and characteristics of materials in various operational circumstances thereby facilitating the enhancement of engine component performance, functionality efficacy, durability, and longevity.

Data availability statement

The original contributions presented in the study are included in the article/Supplementary material, further inquiries can be directed to the corresponding authors.

Author contributions

BS: Conceptualization, Formal Analysis, Investigation, Methodology, Writing–original draft. JS: Conceptualization, Formal Analysis, Investigation, Methodology, Writing–original draft. RK: Conceptualization, Formal Analysis, Investigation, Methodology, Writing–original draft. SS: Conceptualization, Formal Analysis, Funding acquisition, Investigation, Methodology, Project administration, Supervision, Writing–original draft, Writing–review and editing. AK: Conceptualization, Formal Analysis, Investigation, Methodology, Writing–original draft. KM: Conceptualization, Formal Analysis, Investigation, Methodology, Writing–original draft. FA: Funding acquisition, Project administration, Supervision, Writing–review and editing. MK: Funding acquisition, Project administration, Supervision, Writing–review and editing. EI: Funding acquisition, Project administration, Supervision, Writing–review and editing.

Funding

The author(s) declare that no financial support was received for the research, authorship, and/or publication of this article.

Acknowledgments

The authors would like to thank King Saud University, Riyadh, Saudi Arabia, with researchers supporting project number RSPD2023R576.

Conflict of interest

The authors declare that the research was conducted in the absence of any commercial or financial relationships that could be construed as a potential conflict of interest.

Publisher's note

References

Abdou, S., Elkaseer, A., Kouta, H., and Abu Qudeiri, J. (2018). Wear behaviour of grey cast iron with the presence of copper addition. *Adv. Mech. Eng.* 10 (10), 168781401880474. doi:10.1177/1687814018804741

Alemani, M., Gialanella, S., Straffelini, G., Ciudin, R., Olofsson, U., Perricone, G., et al. (2017). Dry sliding of a low steel friction material against cast iron at different loads: characterization of the friction layer and wear debris. *Wear* 376 (377), 1450–1459. doi:10.1016/j.wear.2017.01.040

Bai, X., Zhang, Z., Shi, H., Luo, Z., and Li, T. (2023). Identification of subsurface mesoscale crack in full ceramic ball bearings based on strain energy theory. *Appl. Sci.* 13 (13), 7783. doi:10.3390/app13137783

Campbell, P., Laoui, T., Celis, J., and Der Biest, V. (1996). The influence of intergranular phases on the tribological performance of sialons. *Mater. Sci. Eng. A* 207, 72–86. doi:10.1016/0921-5093(96)80004-9

Chawla, K. K., Saini, N., and Dhiman, R. (2013). Investigation of tribological behavior of stainless steel 304 and grey cast iron rotating against EN32 steel using pin on disc apparatus. *IOSR J. Mech. Civ. Eng.* 9, 18–22. doi:10.9790/1684-0941822

Cheng, Z., Guo, Z., Fu, P., Yang, J., and Wang, Q. (2021). New insights into the effects of methane and oxygen on heat/mass transfer in reactive porous media. *Int. Commun. heat mass Transf.* 129, 105652. doi:10.1016/j.icheatmasstransfer.2021.105652

Cui, X., Li, C., Yang, M., Liu, M., Gao, T., Wang, X., et al. (2023). Enhanced grindability and mechanism in the magnetic traction nanolubricant grinding of Ti-6Al-4 V. *Tribol. Int.* 186, 108603. doi:10.1016/j.triboint.2023.108603

Cui, X., Li, C., Zhang, Y., Ding, W., An, Q., Liu, B., et al. (2022). Comparative assessment of force, temperature, and wheel wear in sustainable grinding aerospace alloy using biolubricant. *Mech. Eng.* 18 (2), 3. doi:10.1007/s11465-022-0719-x

Dikshit, M. K., Singh, S., Pathak, V. K., Saxena, K. K., Agrawal, M. K., Malik, V., et al. (2023). Surface characteristics optimization of biocompatible Ti6Al4V with RCCD and NSGA II using die sinking EDM. *J. Mater. Res. Technol.* 24, 223–235. doi:10.1016/j.jmrt.2023.03.005

Ferreira, J. C. (2002). A study of cast chilled iron processing technology and wear evaluation of hardened gray iron for automotive application. *J. Mater Process Technol.* 121 (1), 94–101. doi:10.1016/S0924-0136(01)01208-0

Fu, Z. H., Yang, B. J., Shan, M. L., Li, T., Zhu, Z. Y., Ma, C. P., et al. (2020). Hydrogen embrittlement behavior of SUS301L-MT stainless steel laser-arc hybrid welded joint localized zones. *Corros. Sci.* 164, 108337. doi:10.1016/j.corsci.2019.108337

Ganeshkumar, S., Singh, B. K., Kumar, S. D., Gokulkumar, S., Sharma, S., Mausam, K., et al. (2022). Study of wear, stress and vibration characteristics of silicon carbide tool inserts and nano multi-layered titanium nitride-coated cutting tool inserts in turning of SS304 steels. *Materials* 15, 7994. doi:10.3390/ma15227994

García, C., Martín, F., Herranz, G., Berges, C., and Romero, A. (2018). Effect of adding carbides on dry sliding wear behaviour of steel matrix composites processed by metal injection moulding. *Wear* 414 (415), 182–193. doi:10.1016/j.wear.2018.08.010

Gill, A. S., Kumar, S., Singh, J., Agarwal, V., and Sharma, S. (2020). A review of recent methods for tool wear reduction in electrical discharge machining. *Surf. Rev. Lett.* 27, 2030002. doi:10.1142/S0218625X20300026

Güneş, A., Ömer Sinan, Ş., Düzcükoğlu, H., Salur, E., Aslan, A., Kuntoğlu, M., et al. (2021a). Optimization study on surface roughness and tribological behavior of recycled cast iron reinforced bronze MMCs produced by hot pressing. *Materials* 14 (12), 3364. doi:10.3390/ma14123364

Güneş, A., Salur, E., Aslan, A., Kuntoğlu, M., Giasin, K., Pimenov, D. Y., et al. (2021b). Towards analysis and optimization for contact zone temperature changes and specific wear rate of metal matrix composite materials produced from recycled waste. *Mater. (Basel)* 14 (18), 5145. doi:10.3390/ma14185145

Guo, K., Gou, G., Lv, H., and Shan, M. (2022). Jointing of CFRP/5083 aluminum alloy by induction brazing: processing, connecting mechanism, and fatigue performance. *Coatings* 12 (10), 1559. doi:10.3390/coatings12101559

Hu, J., Yang, K., Wang, Q., Chen Zhao, Q., Hui Jiang, Y., and Jie Liu, Y. (2023). Ultra-long life fatigue behavior of a high-entropy alloy. *Int. J. Fatigue* 178, 108013. doi:10.1016/j.ijfatigue.2023.108013

Jain, A., Nabeel, A. N., Bhagwat, S., Kumar, R., Sharma, S., Kozak, D., et al. (2023). Fabrication of polypyrrole gas sensor for detection of NH3 using an oxidizing agent and pyrrole combinations: studies and characterizations. *Heliyon* 9, e17611. doi:10.1016/j.heliyon.2023.e17611

Jia, D., Zhang, Y., Li, C., Yang, M., Gao, T., Said, Z., et al. (2022). Lubrication-enhanced mechanisms of titanium alloy grinding using lecithin biolubricant. *Tribol. Int.* 107461 (22), 107461–107462. doi:10.1016/j.triboint.2022.107461

Kiranakumar, V., Ramakrishnaiah, T., Naveen, S., Khan, M., Gunderi, P., Reddy, S., et al. (2022). A review on electrical and gas-sensing properties of reduced graphene oxide-metal oxide nanocomposites. *Biomass Convers. Biorefinery*. doi:10.1007/s13399-022-03258-7

Korkmaz, M. E., Gupta, M. K., Singh, G., Kuntoğlu, M., Patange, A., Demirsoz, R., et al. (2023). Machine learning models for online detection of wear and friction behaviour of biomedical graded stainless steel 316L under lubricating conditions. *Int. J. Adv. Manuf. Technol.* 128 (5-6), 2671–2688. doi:10.1007/s00170-023-12108-3

Kowandy, C., Richard, C., Chen, Y. M., and Tessier, J. J. (2007). Correlation between the tribological behaviour and wear particle morphology-case of grey cast iron 250 versus Graphite and PTFE. *Wear* 262 (7–8), 996–1006. doi:10.1016/j.wear.2006.10.015

Kumar, J., Singh, D., Kalsi, N. S., Sharma, S., Yu Pimenov, D., Venkateswara Rao, K., et al. (2020). Comparative study on the Mechanical, Tribological, Morphological and Structural properties of vortex casting processed, Al-SiC-Cr hybrid metal matrix composites for high strength wear-resistant applications: fabrication and characterizations. *J. Mater. Res. Technol. (JMR&T)* 9, 13607–13615. doi:10.1016/j.jmrt.2020.10.001

Kumar, M. S., Sathisha, N., Manjnatha, S., Niranjana, S. J., Tamam, N., and Khan, M. I. (2023c). Fatigue surface analysis of AL A356 alloy reinforced hematite metal matrix composites. *Biomass Conv. bioref.* doi:10.1007/s13399-023-04634-7

Kumar, R., Dwivedi, R., Arya, R., Sonia, P., Yadav, A., Saxena, K., et al. (2023d). Current development of carbide free bainitic and retained austenite on wear resistance in high silicon steel. *J. Mater. Res. Technol.* 24, 9171–9202. doi:10.1016/j.jmrt.2023.05.067

Kumar, R., Sharma, S., Gulati, P., Singh, J. P., Jha, K., Li, C., et al. (2023a). Fabrication and characterizations of Glass fiber-reinforced functional leaf spring composites with or without microcapsule-based dicyclopentadiene as self-healing agent for automobile industrial applications: comparative analysis. *J. Mater. Res. Technol.* 25, 2797–2814. doi:10.1016/j.jmrt.2023.06.039

Kumar, R., Sharma, S., Singh, J. P., Gulati, P., Singh, G., Prakash Dwivedi, S., et al. (2023b). Enhancement in wear-resistance of 30MNCRB5 Boron steel-substrate using HVOF thermal sprayed WC-10%Co-4%Cr coatings: a comprehensive research on microstructural, tribological, and morphological analysis. *J. Mater. Res. Technol.* 27, 1072–1096. doi:10.1016/j.jmrt.2023.09.265

Kumar, R., Singh, J., Sharma, S., Li, C., Królczyk, G., Eldin, E. M. T., et al. (2022b). Identification of localized defects and fault Size estimation of taper roller bearing (NBC_30205) with signal processing using the Shannon Entropy method in MATLAB for automobile industries applications. *Heliyon* 8, e12053. doi:10.1016/j.heliyon.2022.e12053

Kumar, R., Singh, J., Sharma, S., Li, C., Królczyk, G., and Wojciechowski, S. (2022a). Neutrosophic entropy-based ingenious measurement for fast fourier transforms based classification of process-parameters and wear resistance of friction-stir processed hybrid AA7075- B4C aluminium metal-matrix composites. *J. Mater. Res. Technol.* 20, 720–739. doi:10.1016/j.jmrt.2022.07.026

Lashin, M. M. A., Ibrahim, M. Z., Khan, M. I., Guedri, K., Saxena, K. K., and Eldin, S. M. (2022). Fuzzy control modeling to optimize the hardness and geometry of laser cladded Fe-based MG single track on stainless steel substrate prepared at different surface roughness. *Micromachines* 13 (12), 2191. doi:10.3390/mi13122191

Li, H., Zhang, Y., Li, C., Zhou, Z., Nie, X., Chen, Y., et al. (2022). Extreme pressure and antiwear additives for lubricant: academic insights and perspectives. *Int. J. Adv. Manuf. Technol.* 120, 1–27. doi:10.1007/s00170-021-08614-x

Li, T., Shi, H., Bai, X., Zhang, K., and Bin, G. (2023). Early performance degradation of ceramic bearings by a twin-driven model. *Mech. Syst. Signal Process.* 204, 110826. doi:10.1016/j.ymssp.2023.110826

Liao, D., Zhu, S., Keshtegar, B., Qian, G., and Wang, Q. (2020). Probabilistic framework for fatigue life assessment of notched components under size effects. *Int. J. Mech. Sci.* 181, 105685. doi:10.1016/j.ijmecsci.2020.105685

Liu, L., Fu, S., and Han, C. (2023d). Investigation on diesel spray flame evolution and its conceptual model for large nozzle and high-density of ambient gas. *Fuel* 339, 127357. doi:10.1016/j.fuel.2022.127357

Liu, L., Peng, Y., Zhang, W., and Ma, X. (2023c). Concept of rapid and controllable combustion for high power-density diesel engines. *Energy Convers. Manag.* 276, 116529. doi:10.1016/j.enconman.2022.116529

Liu, M., Li, C., Yang, M., Gao, T., Wang, X., Cui, X., et al. (2023a). Mechanism and enhanced grindability of cryogenic air combined with biolubricant grinding titanium alloy. *Tribol. Int.* 187, 108704. doi:10.1016/j.triboint.2023.108704

Liu, M., Li, C., Zhang, Y., Yang, M., Gao, T., Cui, X., et al. (2023b). Analysis of grain tribology and improved grinding temperature model based on discrete heat source. *Tribol. Int.* 180, 108196. doi:10.1016/j.triboint.2022.108196

Liu, T., Liu, X., and Feng, P. (2020). A comprehensive review on mechanical properties of pultruded FRP composites subjected to long-term environmental effects. *Compos. Part B Eng.* 191, 107958. doi:10.1016/j.compositesb.2020.107958

Masuda, K., Oguma, N., Ishiguro, M., Sakamoto, Y., and Ishihara, S. (2021). Sliding wear life and sliding wear mechanism of gray cast iron AISI NO.35B. *Wear* 474–475, 203870. doi:10.1016/j.wear.2021.203870

Milojević, S., Savić, S., Mitrovic, S., Maric, D., Krstić, B., Stojanovic, B., and Popovic, V. (2023). Solving the problem of friction and wear in auxiliary devices of internal combustion engines on the example of reciprocating air compressor for vehicles. *Teh. Vjesn.* 30 (1), 122–130. doi:10.17559/TV-20220414105757

Milojević, S., Savić, S., Marić, D., Stopka, O., Krstić, B., and Stojanović, B. (2022). Correlation between emission and combustion characteristics with the compression ratio and fuel injection timing in tribologically optimized diesel engine. *Teh. Vjesn.* 29 (4), 1210–1219. doi:10.17559/TV-20211220232130

Miniappan, P. K., Marimuthu, S., Kumar, S. D., Gokilakrishnan, G., Sharma, S., Li, C., et al. (2023). Mechanical, fracture-deformation, and tribology behavior of fillers-reinforced sisal fiber composites for lightweight automotive applications. *Rev. Adv. Mater. Sci.* 62 (1), 20230342. doi:10.1515/rams-2023-0342

Niu, X., Zhu, S., He, J., Liao, D., Correia, J. A. F. O., Berto, F., et al. (2022). Defect tolerant fatigue assessment of AM materials: size effect and probabilistic prospects. *Int. J. Fatigue* 160, 106884. doi:10.1016/j.ijfatigue.2022.106884

Prasad, B. K. (2011). Sliding wear response of a grey cast iron: effects of some experimental parameters. *Tribol. Int.* 44 (5), 660–667. doi:10.1016/j.triboint.2011.01.006

Prasanthi, P., Kumar, M., Mallampati, S., Madhav, V., Saxena, K., Mohammed, K., et al. (2023). Mechanical properties of carbon fiber reinforced with carbon nanotubes and graphene filled epoxy composites: experimental and numerical investigations. *Mater. Res. Express* 10, 025308. doi:10.1088/2053-1591/acaef5

Purohit, R., and Sagar, R. (2010). Fabrication and testing of Al-SiCp composite poppet valve guides. *Int. J. Adv. Manuf. Technol.* 51 (5–8), 685–698. doi:10.1007/s00170-010-2637-z

Rajawat, A. S., Singh, S., Gangil, B., Ranakoti, L., Sharma, S., Asyraf, M. R. M., et al. (2022). Effect of marble dust on the mechanical, morphological, and wear performance of basalt fibre-reinforced epoxy composites for structural applications. *Polymers* 14 (7), 1325. doi:10.3390/polym14071325

Ramakrishnan, P. (2013). "Automotive applications of powder metallurgy," in *Advances in powder metallurgy* (Amsterdam, Netherlands: Elsevier), 493–519. doi:10.1533/9780857098900.4.493

Ranakoti, L., Gangil, B., Rajesh, P. K., Singh, T., Sharma, S., Li, C., et al. (2022). Effect of surface treatment and fiber loading on the physical, mechanical, sliding wear, and morphological characteristics of tasar silk fiber waste-epoxy composites for multifaceted biomedical and engineering applications: fabrication and characterizations. *J. Mater. Res. Technol.* 19, 2863–2876. doi:10.1016/j.jmrt.2022.06.024

Riahi, A. R., and Alpas, A. T. (2003). Wear map for grey cast iron. *Wear* 255 (1–6), 401–409. doi:10.1016/S0043-1648(03)00100-5

Scherge, M., Linsler, D., and Schlarb, T. (2015). The running-in corridor of lubricated metal-metal contacts. *Wear* 342–343, 60–64. doi:10.1016/j.wear.2015.08.014

Sehar, B., Waris, M., Gilani, S., Ansari, U., Mushtaq, S., Khan, N., et al. (2022). The impact of laminations on the mechanical strength of carbon-fiber composites for prosthetic foot fabrication. *Crystals* 12, 1429. doi:10.3390/cryst12101429

Shahid, M., Javed, H. M. A., Ahmad, M., Qureshi, A., Khan, M., Alnuwaiser, M., et al. (2022). A brief assessment on recent developments in efficient electrocatalytic nitrogen reduction with 2D non-metallic nanomaterials. *Nanomater. (Basel, Switz.* 12, 3413. doi:10.3390/nano12193413

Sharma, H., Kumar, A., Rana, S., Sahoo, N. G., Jamil, M., Kumar, R., et al. (2023). Critical review on advancements on the fiber-reinforced composites: role of fiber/matrix modification on the performance of the fibrous composites. *J. Mater. Res. Technol.* 26, 2975–3002. doi:10.1016/j.jmrt.2023.08.036

Shen, D., Cheng, M., Wu, K., Sheng, Z., and Wang, J. (2022). Effects of supersonic nozzle guide vanes on the performance and flow structures of a rotating detonation combustor. *Acta Astronaut.* 193, 90–99. doi:10.1016/j.actaastro.2022.01.002

Shi, H., Song, Z., Bai, X., Hu, Y., Li, T., and Zhang, K. (2023b). A novel digital twin model for dynamical updating and real-time mapping of local defect extension in rolling bearings. *Mech. Syst. Signal Process.* 193, 110255. doi:10.1016/j.ymssp.2023.110255

Shi, J., Zhao, B., He, T., Tu, L., Lu, X., and Xu, H. (2023a). Tribology and dynamic characteristics of textured journal-thrust coupled bearing considering thermal and pressure coupled effects. *Tribol. Int.* 180, 108292. doi:10.1016/j.triboint.2023.108292

Singh, B., Grewal, J. S., and Sharma, S. (2021a). "Effect of addition of flyash and graphite on the mechanical properties of A6061-T6," in *Materials today: proceedings* (Amsterdam, Netherlands: Elsevier Ltd), 2411–2415. doi:10.1016/j.matpr.2021.10.258

Singh, B., Kumar, I., Saxena, K., Mohammed, K., Khan, M., Ben Moussa, S., et al. (2023). A future prospects and current scenario of aluminium metal matrix composites characteristics. *Alexandria Eng. J.* 76, 1–17. doi:10.1016/j.aej.2023.06.028

Singh, J., Gill, S. S., Dogra, M., Sharma, S., Singh, M., Dwivedi, S. P., et al. (2022). Effect of ranque-hilsch vortex tube cooling to enhance the surface-topography and tool-wear in sustainable turning of Al-5.6Zn-2.5Mg-1.6Cu-0.23Cr-T6 aerospace alloy. *Materials* 15 (16), 5681. doi:10.3390/ma15165681

Singh, S. K., Chattopadhyaya, S., Pramanik, A., Kumar, S., ShaileshPandey, M., Walia, R. S., et al. (2021b). Effect of alumina oxide nano-powder on the wear behaviour of CrN coating against cylinder liner using response surface methodology: processing and characterizations. *J. Mater. Res. Technol. (JMR&T)* 16, 1102–1113. doi:10.1016/j.jmrt.2021.12.062

Sipcikoğlu, B. I., Yiğit, B., Oflaz, H., Parlar, Z., and Temiz, V. (2015). The investigation of friction and wear characteristic of cast iron against manganese phosphate coated and austempered compressor crankshaft. *FME Trans.* 43 (3), 186–190. doi:10.5937/fmet1503186S

Skrbek, B., and Mráz, J. (2020). "Sliding couples for valve guides and valves of picton combustion engines," in Proceedings of the METAL 2020 - 29th International Conference on Metallurgy and Materials, Conference Proceedings, Brno, Czech Republic, EU, May 2020 (TANGER Ltd.), 696–701. doi:10.37904/metal.2020.3545

Srivastva, H. K., Chauhan, A. S., Kushwaha, M., Raza, A., Bhardwaj, P., and Raj, V. (2016). Comparative study of different materials with Al-sic for engine valve guide by using FEM. *World J. Eng. Technol.* 04 (02), 238–251. doi:10.4236/wjet.2016.42023

Synák, F., Synák, J., Skrúcaný, T., and Milojević, S. (2019). Modification of engine control unit data and selected vehicle characteristics. *Appl. Eng. Lett.* 4 (4), 120–127. doi:10.18485/aeletters.2019.4.4.3

Terheci, M., Manory, R. R., and Herder, J. H. (1995). The friction and wear of automotive grey cast iron under dry sliding conditions Part 2. Friction and wear-particle generation mechanisms and their progress with time. *Wear* 185, 119–124. doi:10.1016/0043-1648(95)06593-8

Usca, Ü. A., Uzun, M., Kuntoğlu, M., Şap, S., Giasin, K., and Danil Yurievich, P. (2021). Tribological aspects, optimization and analysis of Cu-B-CrC composites fabricated by powder metallurgy. *Powder Metallurgy" Mater.* 14 (15), 4217. doi:10.3390/ma14154217

Vadiraj, A., Balachandran, G., Kamaraj, M., Gopalakrishna, B., and Venkateshwara Rao, D. (2010). Wear behavior of alloyed hypereutectic gray cast iron. *Tribol. Int.* 43 (3), 647–653. doi:10.1016/j.triboint.2009.10.004

Vadiraj, A., Kamaraj, M., and Sreenivasan, V. S. (2011). Wear and friction behavior of alloyed gray cast iron with solid lubricants under boundary lubrication. *Tribol. Int.* 44 (10), 1168–1173. doi:10.1016/j.triboint.2011.05.011

Vemanaboina, H., Babu, M. M., Prerana, I. C., Gundabattini, E., Yelamasetti, B., Saxena, K. K., et al. (2023). Evaluation of residual stresses in CO2 laser beam welding of SS316L weldments using FEA. *Mater. Res. Express* 10 (1), 016509. doi:10.1088/2053-1591/acb0b5

Vladimirova, Y. O., and Shalunov, E. P. (2020). "Development of copper dispersion-strengthened composite material with increased indexes of high erature strength and wear resistance for thermally loaded friction pairs," in *Journal of physics: conference series* (Bristol, England: Institute of Physics Publishing). doi:10.1088/1742-6596/1431/1/012012

Wang, X., Li, C., Zhang, Y., Hafiz Muhammad Ali, S. S., Li, R., Yang, M., et al. (2022). Tribology of enhanced turning using biolubricants: a comparative assessment. *Tribol. Int.* 174, 107766. doi:10.1016/j.triboint.2022.107766

Wu, Y., Liu, L., Liu, B., Cao, E., and Xiong, Q. (2023). Investigation of rapid flame front controlled knock combustion and its suppression in natural gas dual-fuel marine engine. *Energy* 279, 128078. doi:10.1016/j.energy.2023.128078

Xu, J., Liu, J., Zhang, Z., and Wu, X. (2023). Spatial-temporal transformation for primary and secondary instabilities in weakly non-parallel shear flows. *J. Fluid Mech.* 959, A21. doi:10.1017/jfm.2023.67

Yadav, V., Singh, S., Chaudhary, N., Garg, M., Sharma, S., Kumar, A., et al. (2023). Dry sliding wear characteristics of natural fibre reinforced poly-lactic acid composites for Engineering applications: fabrication, properties and characterizations. *J. Mater. Res. Technol.* 23, 1189–1203. doi:10.1016/j.jmrt.2023.01.006

Yu, H., Zhang, J., Fang, M., Ma, T., Wang, B., Zhang, Z., et al. (2023a). Bio-inspired strip-shaped composite composed of glass fabric and waste selvedge from *A. pernyi* silk for lightweight and high-impact applications. *Compos. Part A Appl. Sci. Manuf.* 174, 107715. doi:10.1016/j.compositesa.2023.107715

Yu, J., Shi, Z., Dong, X., Li, Q., Lv, J., and Ren, Z. (2023b). Impact time consensus cooperative guidance against the maneuvering target: theory and experiment. *IEEE Trans. Aerosp. Electron. Syst.* 59 (4), 4590–4603. doi:10.1109/TAES.2023.3243154

Zhao, P., Zhu, J., Yang, K., Li, M., Shao, G., Lu, H., et al. (2023). Outstanding wear resistance of plasma sprayed high-entropy monoboride composite coating by inducing phase structural cooperative mechanism. *Appl. Surf. Sci.* 616, 156516. doi:10.1016/j.apsusc.2023.156516

Zhou, W., Northwood, D. O., and Liu, C. (2021). A steel-like unalloyed multiphase ductile iron. *J. Mater. Res. Technol.* 15, 3836–3849. doi:10.1016/j.jmrt.2021.10.021

Zhu, Q., Chen, J., Gou, G., Chen, H., and Li, P. (2017). Ameliorated longitudinal critically refracted—attenuation velocity method for welding residual stress measurement. *J. Mater. Process. Technol.* 246, 267–275. doi:10.1016/j.jmatprotec.2017.03.022

Zhu, Z. Y., Liu, Y. L., Gou, G. Q., Gao, W., and Chen, J. (2021). Effect of heat input on interfacial characterization of the butter joint of hot-rolling CP-Ti/Q235 bimetallic sheets by Laser + CMT. *Sci. Rep.* 11 (1), 10020. doi:10.1038/s41598-021-89343-9